

**Hubble expansion and structure formation in time varying vacuum models**Spyros Basilakos,<sup>1</sup> Manolis Plionis,<sup>2</sup> and Joan Solà<sup>3</sup><sup>1</sup>*Academy of Athens, Research Center for Astronomy and Applied Mathematics, Soranou Efessiou 4, 11527, Athens, Greece*<sup>2</sup>*Institute of Astronomy & Astrophysics, National Observatory of Athens, Thessio 11810, Athens, Greece  
and Instituto Nacional de Astrofísica, Óptica y Electrónica, 72000 Puebla, Mexico*<sup>3</sup>*High Energy Physics Group, Departament Estructura i Constituents de la Matèria, Universitat de Barcelona,  
Diagonal 647, 08028 Barcelona, Catalonia, Spain**and Institut de Ciències del Cosmos, Univ. de Barcelona, Barcelona*

(Received 27 July 2009; published 8 October 2009)

We investigate the properties of the FLRW flat cosmological models in which the vacuum energy density evolves with time,  $\Lambda(t)$ . Using different versions of the  $\Lambda(t)$  model, namely, quantum field vacuum, power series vacuum and power law vacuum, we find that the main cosmological functions such as the scale factor of the Universe, the Hubble expansion rate  $H$ , and the energy densities are defined analytically. Performing a joint likelihood analysis of the recent supernovae type Ia data, the cosmic microwave background shift parameter and the baryonic acoustic oscillations traced by the Sloan Digital Sky Survey galaxies, we put tight constraints on the main cosmological parameters of the  $\Lambda(t)$  scenarios. Furthermore, we study the linear matter fluctuation field of the above vacuum models. We find that the patterns of the power series vacuum  $\Lambda = n_1 H + n_2 H^2$  predict stronger small scale dynamics, which implies a faster growth rate of perturbations with respect to the other two vacuum cases (quantum field and power law), despite the fact that all the cosmological models share the same equation of state parameter. In the case of the quantum field vacuum  $\Lambda = n_0 + n_2 H^2$ , the corresponding matter fluctuation field resembles that of the traditional  $\Lambda$  cosmology. The power law vacuum ( $\Lambda \propto a^{-n}$ ) mimics the classical quintessence cosmology, the best fit being tilted in the phantom phase. In this framework, we compare the observed growth rate of clustering measured from the optical galaxies with those predicted by the current  $\Lambda(t)$  models. Performing a Kolmogorov-Smirnov statistical test we show that the cosmological models which contain a constant vacuum ( $\Lambda$ CDM), quantum field vacuum, and power law vacuum provide growth rates that match well with the observed growth rate. However, this is not the case for the power series vacuum models (in particular, the frequently adduced  $\Lambda \propto H$  model) in which clusters form at significantly earlier times ( $z \geq 4$ ) with respect to all other models ( $z \sim 2$ ). Finally, we derived the theoretically predicted dark matter halo mass function and the corresponding distribution of cluster-size halos for all the models studied. Their expected redshift distribution indicates that it will be difficult to distinguish the closely resembling models (constant vacuum, quantum field, and power law vacuum), using realistic future x-ray surveys of cluster abundances. However, cluster surveys based on the Sunayev-Zeldovich detection method give some hope to distinguish the closely resembling models at high redshifts.

DOI: 10.1103/PhysRevD.80.083511

PACS numbers: 98.80.-k, 95.35.+d, 95.36.+x

**I. INTRODUCTION**

Over the past decade, studies of the available high quality cosmological data [supernovae type Ia, cosmic microwave background (CMB), galaxy clustering, etc.] have converged towards a cosmic expansion history that involves a spatially flat geometry and a recent accelerating expansion of the Universe (cf. [1–6] and references therein). This expansion has been attributed to an energy component called dark energy (DE) with negative pressure, which dominates the universe at late times. The simplest type of DE corresponds to the cosmological constant (see [7–9] for reviews). The so-called concordance model (or  $\Lambda$ CDM model), which contains cold dark matter (DM) to explain clustering, flat spatial geometry, and a cosmological constant,  $\Lambda$ , fits accurately the current observational data and thus it is an excellent candidate to be

the model that describes the observed universe. However, the concordance model suffers from, among others [10], two fundamental problems: (a) *The “old” cosmological constant problem (or fine tuning problem)* i.e., the fact that the observed value of the vacuum energy density ( $\rho_\Lambda = \Lambda c^2/8\pi G \simeq 10^{-47} \text{ GeV}^4$ ) is many orders of magnitude below the value found using quantum field theory (QFT) [7], and (b) *the coincidence problem* [11] i.e., the fact that the matter energy density and the vacuum energy density are of the same order just prior to the present epoch, despite the fact that the former is a rapidly decreasing function of time while the latter is just stationary. The extremal possibility concerning problem (a) occurs when the Planck mass  $M_P \sim 10^{19} \text{ GeV}$  is used as the fundamental scale; then the ratio  $M_P^4/\rho_\Lambda$  becomes  $\sim 10^{123}$ . One may think that physics at the Planck scale is not well under control and that this

enormous ratio might be fictitious. However, let us consider the more modest scale  $v = 2M_W/g \simeq 250$  GeV associated to the electroweak standard model (SM) of particle physics (the experimentally most successful QFT known to date), where  $M_W$  and  $g$  are the  $W^\pm$  boson mass and the  $SU(2)$  gauge coupling, respectively. In this case, the ratio of the predicted vacuum energy versus the measured one is still very large: it reads  $|\langle V \rangle|/\rho_\Lambda \gtrsim 10^{55}$ , where  $\langle V \rangle = -(1/8)M_H^2 v^2$  is the vacuum expectation value of the Higgs potential and  $M_H \gtrsim 114.4$  GeV is the lower bound on the Higgs boson mass in the SM.

Attempts to solve the above problems have been presented in the literature (see [8,9,12] and references therein). Historically, the first attempts to solve the “old  $\Lambda$  problem” (the toughest one in the list) were based on dynamical adjustment mechanisms [13] aiming to avoid a mere fine tuning of the various QFT contributions. Later on it was realized that a dynamical  $\Lambda$  could also be useful to overpass the coincidence problem. The idea is to replace the constant vacuum energy either with a DE that evolves with time (quintessence and the like [8]), or alternatively with a time varying vacuum energy density,  $\rho_\Lambda(t)$  (cf. [14,15]). In the quintessence context, one can introduce an *ad hoc* tracker scalar field  $\phi$  [16] (different from the usual SM Higgs field) rolling down the potential energy  $V(\phi)$ , and therefore it could resemble the DE. Detailed analysis of these models exist in the literature, including their confrontation with the data [17–20]—see also [8,9,21] for extensive reviews. Nevertheless, the idea of a scalar field rolling down some suitable potential does not really solve the problem because the initial value of the DE still needs to be fine tuned. Moreover, the typical mass of  $\phi$  is usually very small. Indeed, being  $\phi$  unrelated to the SM physics, it is usually thought of as a high energy field  $\langle \phi \rangle \simeq M_X$  where  $M_X$  is some scale near the Planck mass. If one assumes the simplest form for its potential, namely,  $V(\phi) = m_\phi^2 \phi^2/2$ , and requires it to reproduce the present value of the vacuum energy density,  $\rho_\Lambda = \langle V(\phi) \rangle \sim 10^{-11}$  eV<sup>4</sup>, the mass of  $\phi$  is predicted in the ballpark of  $m_\phi \sim H_0 \sim 10^{-33}$  eV. This is an inconceivably small mass scale in particle physics. Thus, the problem that one is creating along with the introduction of  $\phi$  is much bigger than the problem that one is intending to solve, for one is postulating a mass scale which is 30 orders of magnitude below the mass scale  $m_\Lambda$  associated to the value of the vacuum energy density  $m_\Lambda \equiv \rho_\Lambda^{1/4} \sim 2.3 \times 10^{-3}$  eV.

Current observations do not rule out the possibility of a dynamical DE [1–6]. They indicate that the dark energy equation of state (EOS) parameter  $w \equiv P_{\text{DE}}/\rho_{\text{DE}}$  is close to  $-1$  to within  $\pm 10\%$ , if it is assumed to be constant, while it is much more poorly constrained if it varies with time [2]. Let us note, interestingly enough, that models with running vacuum energy, may appear in practice with a nontrivial “effective EOS”  $w = w(t)$  [22], which can be

accommodated by observations. Indeed, the basic feature in this cosmological ideology is that, although the EOS parameter of the vacuum energy is strictly equal to  $-1$ , a time evolving  $\Lambda$  generally results in an effective EOS, usually a function  $w = w(a)$  of the scale factor that approaches  $w \rightarrow -1$  at the present time. This effective EOS may be the result either of the fact that we are trying to describe the variable  $\Lambda(t)$  model as if it were a quintessence-type model with conserved DE [22], or of the existence of other DE entities mixed up with the variable  $\Lambda(t)$ , as e.g. in the case of the  $\Lambda$ XCDM model [14,23].

Although the precise functional form of  $\Lambda(t)$  is still missing, an interesting QFT approach within the context of the renormalization group (RG) was proposed long ago [24,25]. Later on, the RG-running framework was further explored in [26] from the viewpoint of QFT in curved space-time by employing the standard perturbative RG-techniques of particle physics (see also [27] for a functional RG approach in a nonperturbative context). A more phenomenological point of view was addressed in [28], in which a time varying  $\Lambda(t)$  parameter could be a possible candidate to solve the two fundamental cosmological puzzles. There is an extensive literature on time varying  $\Lambda$  models (cf. [29–31] and references therein).

It is worth noticing, that for an important class of  $\Lambda(t)$  models there is a coupling between the time-dependent vacuum and matter. A first work confronting supernovae data with a (RG-inspired [26]) model of this kind was presented in [32]—see also [33]. Using the combination of the conservation of the total energy with the variation of the vacuum energy, one can show that these  $\Lambda(t)$  models provide either a particle production process or that the mass of the dark matter particles increases. Despite the fact that most of the recent papers on these matters are based on the assumption that the DE evolves independently of the dark matter, the unknown nature of the DE and DM implies that at the moment we can not exclude the possibility of interactions in the dark sector, whether at the level of a variable  $\Lambda(t)$  [32,33] or from coupled quintessence [34]. Another possibility is that matter is strictly conserved and that both  $\Lambda(t)$  and the gravitational coupling  $G(t)$  are running [35,36], but this option will not be scrutinized here.

The scope of the present work is to study the observational consequences of the overall dynamics for a wide class of time varying vacuum energy models, in interaction with matter, in the light of the most recent cosmological data. The structure of the paper is as follows. The basic theoretical elements of the problem are presented in Sec. II, where we introduce [for a spatially flat Friedmann-Lemaître-Robertson-Walker (FLRW) geometry] the basic cosmological equations. In Secs. III and IV we place constraints on the main parameters of our vacuum models by performing a joint likelihood analysis utilizing

the so-called ‘‘Constitution set’’ of the supernovae type Ia (SNIa) data [5], the shift parameter of the cosmic microwave background [3] and the observed baryonic acoustic oscillations (BAOs; [37]). Also, we investigate whether the current vacuum cosmological models can yield a late accelerated phase of the cosmic expansion. In Sec. V we compare the observed linear growth rate of clustering measured from the Sloan Digital Sky Survey (SDSS) galaxies with those predicted by the  $\Lambda(t)$  models, explored here, while in Sec. VI we present the corresponding theoretical predictions regarding the formation of the galaxy clusters and the evolution of their abundance. In Sec. VII we draw our conclusions. Note, that throughout the paper we use  $H_0 = 70.5$  km/sec/Mpc [3,38].

## II. COSMOLOGY WITH A TIME DEPENDENT VACUUM

In the framework of a spatially flat FLRW geometry the basic equations which govern the global dynamics of the universe are

$$\rho_m + \rho_\Lambda = 3H^2 \quad (1)$$

and

$$\dot{\rho}_m + \dot{\rho}_\Lambda + 3H(\rho_m + P_m + \rho_\Lambda + P_\Lambda) = 0, \quad (2)$$

where  $\rho_m$  is the matter energy density and  $\rho_\Lambda$  is the vacuum energy density, while  $P_m$  and  $P_\Lambda$  are the corresponding matter and vacuum pressures. Notice, that in order to simplify our formalism we use geometrical units ( $8\pi G = c \equiv 1$ ) in which  $\rho_\Lambda = \Lambda$ .

In the present work, we would like to investigate the potential of a time varying  $\Lambda = \Lambda(t)$  parameter to account for the observed acceleration of the expansion of the Universe. Within this framework it is interesting to mention that the equation of state takes the usual form  $P_\Lambda(t) = -\rho_\Lambda(t) = -\Lambda(t)$ , and we remark that this EOS does not depend on whether  $\Lambda$  is strictly constant or variable. Also, by introducing in the global dynamics the idea of the time-dependent vacuum, it is possible to explain the physical properties of the DE as well as to ameliorate the status of the fine tuning and the coincidence problem, respectively. In the matter dominated epoch ( $P_m = 0$ ), Eq. (2) leads to the following useful formula:

$$\dot{\rho}_m + 3H\rho_m = -\dot{\Lambda}, \quad (3)$$

and considering Eq. (1), we find

$$\dot{H} + \frac{3}{2}H^2 = \frac{\Lambda}{2}, \quad (4)$$

where the over-dot denotes derivatives with respect to the cosmic time. If the vacuum term is negligible,  $\Lambda(t) \rightarrow 0$ , then the solution of the above equation reduces to that of the Einstein de Sitter model,  $H(t) = 2/3t$ , as it should. Obviously, if we consider the case of  $\Lambda(t) \neq 0$ , then it

becomes evident—see Eq. (3)—that there is a coupling between the time-dependent vacuum and matter component. This equation was first considered by M. Bronstein in a rather old paper [39]. Note, that the traditional  $\Lambda = \text{const}$  cosmology (or  $\Lambda$ CDM model) can be described directly by the integration of the Eq. (4) [for more details see Sec. IVA], but this same equation is also valid for  $\Lambda = \Lambda(t)$ , in which case a supplementary equation for the time evolution of  $\Lambda$  is needed in order to unveil the dynamics of this model. As we have already stated before, the link in Eq. (3) between  $\dot{\rho}_m$  and  $\dot{\Lambda}$  is very important because interactions between DM and DE could provide possible solutions to the cosmological coincidence problem. This is the reason for which several papers have been published recently in this area [34] proposing that the DE and DM could be coupled. Alternatively, one may use a variable  $\Lambda$  together with another entity  $X$ , that ensures a total self-conserved DE density,  $\rho_{\text{DE}} = \rho_\Lambda + \rho_X$ , such that the ratio  $\rho_{\text{DE}}/\rho_m$  remains fairly stable for most of the Universe’s lifetime [14]. In both cases a time-dependent DE is needed.

In the following, we are going to concentrate on models where the time dependence of  $\Lambda$  appears always at the expense of an interaction with matter. In this context, the corresponding time evolution equation for the matter density contrast  $D \equiv \delta\rho_m/\rho_m$ , in a pressureless fluid, is given by [40]

$$\ddot{D} + (2H + Q)\dot{D} - \left[ \frac{\rho_m}{2} - 2HQ - \dot{Q} \right] D = 0, \quad (5)$$

where

$$\rho_m = 3H^2 - \Lambda \quad Q(t) = -\dot{\Lambda}/\rho_m. \quad (6)$$

It becomes clear, that the interacting vacuum energy affects the growth factor via the function  $Q(t)$ . Of course, in order to solve the above differential equations we need to define explicitly the functional form of the  $\Lambda(t)$  component. Notice that the approach based on Eq. (5) effectively implies that the DE perturbations are negligible (i.e., in this case we set  $\delta\Lambda = 0$ ). This is justified in most cases, specially for perturbations well inside the sound horizon (of the dark energy medium) where it behaves very smoothly [41,42]. In fact, one can explicitly derive Eq. (5) starting from the general coupled set of matter and dark energy perturbations [see Eqs. (17), (25), and (27) of Ref. [41], which we refrain from repeating here]. Assuming that matter and  $\Lambda(t)$  interact as in Eq. (3), taking the limit where the DE perturbations are neglected, and assuming also that the produced particles of matter have negligible velocities with respect to the comoving observers, then the aforesaid coupled set of matter and DE perturbation equations lead to a second order differential equation for  $D$  that boils down to Eq. (5) above. In this way, we can state that this effective equation follows from the general relativistic treatment of perturbations, within the aforementioned set of approximations, whereas in [40]

it was originally proven directly within the Newtonian formalism.

### III. LIKELIHOOD ANALYSIS

In this work, we use a variety of cosmologically relevant observations in order to constrain the vacuum models explored here (see Sec. IV). These are:

- (i) *Baryonic acoustic oscillations (BAOs)*: These are produced by pressure (acoustic) waves in the photon-baryon plasma in the early universe, generated by dark matter overdensities. Evidence of this excess was recently found in the clustering properties of the luminous SDSS red galaxies [37] and it can provide a “standard ruler” with which we can constraint the dark energy models. In particular, we use the following estimator [37]:

$$A(\mathbf{p}) = \frac{\sqrt{\Omega_m}}{[z_s^2 E(a_s)]^{1/3}} \left[ \int_{a_s}^1 \frac{da}{a^2 E(a)} \right]^{2/3}, \quad (7)$$

measured from the SDSS data to be  $A = 0.469 \pm 0.017$ , with  $z_s = 0.35$  [or  $a_s = (1 + z_s)^{-1} \simeq 0.75$ ] and  $E(a) \equiv H(a)/H_0$  is the normalized Hubble flow. Therefore, the corresponding  $\chi_{\text{BAO}}^2$  function is simply written

$$\chi_{\text{BAO}}^2(\mathbf{p}) = \frac{[A(\mathbf{p}) - 0.469]^2}{0.017^2}, \quad (8)$$

where  $\mathbf{p}$  is a vector containing the cosmological parameters that we want to fit.

- (ii) *CMB shift parameter*: A very accurate and deep geometrical probe of dark energy is the angular scale of the sound horizon at the last scattering surface as encoded in the location  $l_1^{TT}$  of the first peak of the cosmic microwave background (CMB) temperature perturbation spectrum. This probe, called CMB shift parameter [43–45], is defined as

$$R = \sqrt{\Omega_m} \int_{a_s}^1 \frac{da}{a^2 E(a)}. \quad (9)$$

Note, that the Hubble function  $H(a)$  includes also the radiation component ( $\Omega_r \simeq 10^{-4}$ ). The shift parameter measured from the WMAP 5-years data [3] is  $R = 1.71 \pm 0.019$  at  $z_{ls} = 1090$  [or  $a_{ls} = (1 + z_{ls})^{-1} \simeq 9.17 \times 10^{-4}$ ]. In this case, the  $\chi_{\text{cmb}}^2$  function is given by

$$\chi_{\text{cmb}}^2(\mathbf{p}) = \frac{[R(\mathbf{p}) - 1.71]^2}{0.019^2}. \quad (10)$$

Note that the measured CMB shift parameter is somewhat model dependent but mostly to models which are not included in our analysis. For example, in the case where massive neutrinos are included or when there is a strongly varying equation of state

parameter. The robustness of the shift parameter was tested and discussed in [46].

- (iii) *SNIa distance moduli*: We additionally utilize the “Constitution set” of 397 type Ia supernovae of Hicken *et al.* [5]. In order to avoid possible problems related with the local bulk flow, we use a subsample of the overall sample in which we select those SNIa with  $z > 0.023$ . This subsample contains 351 entries. The corresponding  $\chi_{\text{SNIa}}^2$  function is

$$\chi_{\text{SNIa}}^2(\mathbf{p}) = \sum_{i=1}^{351} \left[ \frac{\mu^{\text{th}}(a_i, \mathbf{p}) - \mu^{\text{obs}}(a_i)}{\sigma_i} \right]^2. \quad (11)$$

where  $a_i = (1 + z_i)^{-1}$  is the observed scale factor of the Universe,  $z_i$  is the observed redshift,  $\mu$  is the distance modulus corresponding to flat space:

$$\mu = m - M = 5 \log d_L + 25 \quad (12)$$

and  $d_L(a, \mathbf{p})$  is the luminosity distance

$$d_L(a, \mathbf{p}) = \frac{c}{a} \int_a^1 \frac{dy}{y^2 H(y)}. \quad (13)$$

Note, that  $c$  is the speed of light ( $c \equiv 1$  here).

We can combine the above cosmologically tests, using a joint likelihood analysis, in order to put even more stringent constraints on the free parameter space, according to:

$$\mathcal{L}_{\text{tot}}(\mathbf{p}) = \mathcal{L}_{\text{BAO}} \times \mathcal{L}_{\text{cmb}} \times \mathcal{L}_{\text{SNIa}}$$

or

$$\chi_{\text{tot}}^2(\mathbf{p}) = \chi_{\text{BAO}}^2 + \chi_{\text{cmb}}^2 + \chi_{\text{SNIa}}^2, \quad (14)$$

with the likelihood estimator defined as  $\mathcal{L}_j \propto \exp[-\chi_j^2/2]$ . Note, that we sample the  $\Omega_m$  parameter in steps of 0.01 in the range [0.1,1] and that the likelihoods are normalized to their maximum values. We will report  $1\sigma$  uncertainties of the fitted parameters. Note that the overall number of data points used is  $N_{\text{tot}} = 353$  and the degrees of freedom:  $\text{dof} = N_{\text{tot}} - n_{\text{fit}}$ , with  $n_{\text{fit}}$  the number of fitted parameters, which vary for the different models.

### IV. CONSTRAINTS ON THE TIME EVOLVING VACUUM MODELS IN FLAT SPACE

As we have already mentioned, the exact nature of a possible time varying vacuum has yet to be found. A large number of different phenomenological parametrizations have appeared in the literature treating the time-dependent  $\Lambda(t)$  function. For example, the authors of [29] considered  $\Lambda(t) = 3\gamma H^2$ , with the constant  $\gamma$  being the ratio of the vacuum to the sum of vacuum and matter density (see also [40]), while [28,47] proposed a different ansatz in which  $\Lambda(t) \propto a^{-2}$ . Also, several papers, (see for example [33,48] and references therein) have investigated the global dynamical properties of the universe considering that the vacuum energy density decreases linearly with the matter

energy density,  $\Lambda \propto \rho_m$ . Carneiro *et al.* [49,50] used a different pattern in which the vacuum term is proportional to the Hubble parameter,  $\Lambda(a) \propto H(a)$ , while [51] considered a power series form in  $H$ . Attempts to provide a theoretical explanation for a dynamical  $\Lambda(t)$  have also been presented in the literature using the renormalization group (RG) in quantum field theory (see [14,26,27,35] and references therein). The RG-inspired form for a QFT running vacuum in curved space-time is

$$\Lambda(H) = n_0 + n_2 H^2, \quad (15)$$

where  $n_0$  and  $n_2$  are constants. This evolution law can mimic the quintessence or phantom behavior [52] as well as a smoothly transition between the two [22]. Notice, that the functional form of Eq. (15) has been also used in [15]. Such a form is indeed crucially different from just considering that the vacuum energy is proportional to  $H^2$ , in the sense that the former is an ‘‘affine quadratic law’’ ( $n_0 \neq 0$ ). Remarkably, the structure of Eq. (15) can be motivated from the QFT framework of anomalous induced inflation (cf. [36] and references therein). In another vein, the aforementioned possibility that the vacuum energy could be evolving linearly with  $H$  has been motivated theoretically in the literature through a possible connection of cosmology with the QCD scale of strong interactions [53]. This option, however, is not what one would expect from renormalizable QFT in curved space-time because from general covariance we should rather expect even powers of  $H$ , as e.g. in the law (15). There is, however, the possibility to add nonanalytic terms in the effective action (see [54] for a recent and interesting attempt in this direction). Such a linear dependence in  $H$  has also been proposed from a possible link of DE with QCD and the topological structure of the universe [55]. Let us, however, note that a connection with QCD can also be achieved through a relaxation mechanism of  $\Lambda$  and without using the hypothesis of linearity in  $H$ —see [23].

In this work, we consider a large family of flat vacuum models and with the aid of the current observational data (see Sec. II) we attempt to put stringent constraints on their free parameters. Also, we investigate thoroughly the time evolution equation of the mass density contrast in the linear regime as well as the formation of galaxy clusters and the evolution of their abundance. In the following subsections, we briefly present these cosmological models which trace differently the vacuum component.

### A. The standard $\Lambda$ cosmology

Without wanting to appear too pedagogical, we remind the reader of some basic elements of the concordance  $\Lambda$  cosmology in order to appreciate the differences with the  $\Lambda(t)$  models explored subsequently. The vacuum term in Eq. (4) is constant and given by  $\Lambda = 3\Omega_\Lambda H_0^2$ . Therefore, it is a routine to integrate Eq. (4) and obtain the Hubble function

$$H(t) = \sqrt{\Omega_\Lambda} H_0 \coth\left(\frac{3H_0\sqrt{\Omega_\Lambda}}{2} t\right), \quad (16)$$

where  $\Omega_\Lambda = 1 - \Omega_m$ . Note, that  $\Omega_m$  is the matter density parameter at the present time. Using now the definition of the Hubble parameter  $H \equiv \dot{a}/a$ , the scale factor of the universe  $a(t)$ , normalized to unity at the present epoch, evolves with time as

$$a(t) = \left(\frac{\Omega_m}{\Omega_\Lambda}\right)^{1/3} \sinh^{2/3}\left(\frac{3H_0\sqrt{\Omega_\Lambda}}{2} t\right). \quad (17)$$

The cosmic time is related with the scale factor as

$$t(a) = \frac{2}{3\sqrt{\Omega_\Lambda} H_0} \sinh^{-1}\left(\sqrt{\frac{\Omega_\Lambda}{\Omega_m}} a^{3/2}\right). \quad (18)$$

Combining the above equations we can define the normalized Hubble expansion as a function of the scale factor

$$E^2(a) = \frac{H^2(a)}{H_0^2} = \Omega_\Lambda + \Omega_m a^{-3}. \quad (19)$$

The inflection point [namely, the point where the Hubble expansion changes from the decelerating to the accelerating regime,  $\ddot{a}(t_I) = 0$ ] takes place at

$$t_I = \frac{2}{3\sqrt{\Omega_\Lambda} H_0} \sinh^{-1}\left(\sqrt{\frac{1}{2}}\right), \quad a_I = \left[\frac{\Omega_m}{2\Omega_\Lambda}\right]^{1/3}. \quad (20)$$

Comparing the concordance model with the observational data we find that the best fit value, within the  $1\sigma$  uncertainty, is  $\Omega_m = 0.28 \pm 0.01$  with  $\chi_{\text{tot}}^2(\Omega_m) \simeq 431.2$  (dof = 352), which is in good agreement with recent studies [1–3,5,6]. Therefore, the current age of the universe is  $t_0 \simeq 13.9$  Gyr while the inflection point is located at  $t_I \simeq 0.52t_0$ ,  $a_I \simeq 0.58$  (hence at redshift  $z_I \simeq 0.72$ ). Let us mention that some recent (approximately model-independent) determinations of this point suggest it to lie at a more recent time (lower redshift) [56], although the results are still compatible with the  $\Lambda$ CDM value within  $2\sigma$ .

Finally, solving Eq. (5) for the  $\Lambda$  cosmology [ $Q(t) = -\dot{\Lambda}/\rho_m = 0$ ], we derive the well known perturbation growth factor (see [57])

$$D(a) = \frac{5\Omega_m E(a)}{2} \int_0^a \frac{dx}{x^3 E^3(x)}. \quad (21)$$

In particular, for  $E(a) = \Omega_m^{1/2} a^{-3/2}$  it gives the standard result  $D(a) = a$ , which corresponds to the matter dominated epoch, as expected. Notice, that (21) is normalized to unity at the present time,  $t_0$ , because in our convention  $a(t_0) = 1$ —cf. Eqs. (17),(18).

### B. The $\Lambda(t)$ model from quantum field theory

Let us consider the vacuum solution (15) proposed in [26,32,35,36] using the renormalization group (RG) in

quantum field theory (hereafter  $\Lambda_{\text{RG}}$  model). We select the coefficients in that equation as  $n_0 = 3H_0^2(\Omega_\Lambda - \gamma)$  and  $n_2 = 3\gamma$ . Therefore,

$$\Lambda(H) = \Lambda_0 + 3\gamma(H^2 - H_0^2). \quad (22)$$

In this way, the vacuum energy density is normalized to the present value  $\Lambda_0 \equiv \Lambda(H_0) = 3\Omega_\Lambda H_0^2$ . Without going into the details of that model, let us recall that  $\gamma$  (called  $\nu$  in the above papers) is interpreted in the RG framework as a “ $\beta$  function” of QFT in curved space-time, which determines the running of the cosmological constant. The predicted value is

$$\gamma = \frac{\sigma}{12\pi} \frac{M^2}{M_P^2}, \quad (23)$$

where  $M_P$  is the Planck mass and  $M$  is an effective mass parameter representing the average mass of the heavy particles of the Grand Unified Theory (GUT) near the Planck scale, after taking into account their multiplicities. Since  $\sigma = \pm 1$  (depending on whether bosons or fermions dominate in the loop contributions), the coefficient  $\gamma$  can be positive or negative, but  $|\gamma|$  is naturally predicted to be much less than one. For instance, if GUT fields with masses  $M_i$  near  $M_P$  do contribute, then  $|\gamma| \lesssim 1/(12\pi) \simeq 2.6 \times 10^{-2}$ , but we expect it to be lesser in practice because the usual GUT scales are not that close to  $M_P$ . By counting particle multiplicities in a typical GUT, a natural estimate is the range  $\gamma = 10^{-5} - 10^{-3}$  (see [36] for details).

We will assume here that  $\Lambda$  evolves in the form (22) while it interacts with matter as in Eq. (3). Alternatively, one may use a variable  $\Lambda$  of the form (22) that interacts with a variable gravitational constant,  $G = G(t)$ , such that matter is conserved (see [35,36]), but we shall not deal with this option here because we wish to consider only the class of variable  $\Lambda$  models in interaction with matter.

It is important to emphasize that the main motivation for the evolution law Eq. (22) stems from the general covariance of the effective action in QFT in curved space-time [26,35,36]—for a review, see e.g. [58]. One expects that deviations from a strictly constant vacuum energy appear as a result of having a nontrivial external metric that describes an expanding FLRW background. Since the expansion rate of this background is  $H$ , we expect a power series in  $H$ . However, for a renormalizable formulation of the effective action of the vacuum, only even powers of the expansion rate  $H$  can appear, the leading correction being of  $\mathcal{O}(H^2)$ . The next-to-leading term would be of  $\mathcal{O}(H^4)$ , the subsequent one of  $\mathcal{O}(H^6/M^2)$ , etc. At the present time, all of the higher order corrections are phenomenologically irrelevant compared to the first curvature correction  $\sim \mathcal{O}(H^2)$  in Eq. (22). Therefore, it is natural to take just the leading form, as in Eq. (22). See, however, [59] for a possible effect of  $H^4$  terms evaluated at the electroweak crossover scale.

It is interesting to point out that the  $\Lambda_{\text{RG}}$  model can be used in different formulations where it helps to alleviate the cosmic coincidence problem [14,15]. It could also have a bearing on the fine tuning problem [15].

From Eqs. (4) and (22) we can easily derive the corresponding Hubble flow as a function of time:

$$H(t) = H_0 \sqrt{\frac{\Omega_\Lambda - \gamma}{1 - \gamma}} \coth \left[ \frac{3}{2} H_0 \sqrt{(\Omega_\Lambda - \gamma)(1 - \gamma)} t \right]. \quad (24)$$

The scale factor of the universe  $a(t)$ , evolves with time as

$$a(t) = a_1 \sinh^{2/3(1-\gamma)} \left[ \frac{3}{2} H_0 \sqrt{(\Omega_\Lambda - \gamma)(1 - \gamma)} t \right], \quad (25)$$

where

$$a_1 = \left( \frac{\Omega_m}{\Omega_\Lambda - \gamma} \right)^{1/3(1-\gamma)}. \quad (26)$$

Inverting Eq. (25) we determine the cosmic time as a function of the scale factor

$$t(a) = \frac{2}{3H_0 \sqrt{(\Omega_\Lambda - \gamma)(1 - \gamma)}} \sinh^{-1} \left[ \left( \frac{a}{a_1} \right)^{3(1-\gamma)/2} \right]. \quad (27)$$

The age of the universe is simply given by this expression at  $a = 1$ , namely, at the point  $t_0 = t(a = 1)$ . The cosmic time at the inflection point of the universe evolution [ $\ddot{a}(t_I) = 0$ ] is found to be

$$t_I = \frac{2}{3H_0 \sqrt{(\Omega_\Lambda - \gamma)(1 - \gamma)}} \sinh^{-1} \left( \sqrt{\frac{1 - 3\gamma}{2}} \right), \quad (28)$$

and the corresponding value of the scale factor reads

$$a_I = \left[ \frac{(1 - 3\gamma)\Omega_m}{2(\Omega_\Lambda - \gamma)} \right]^{1/3(1-\gamma)}. \quad (29)$$

It becomes clear, that for  $\gamma < 1/3$  (this parameter is expected to be very small in QFT) and for the usual values of  $\Omega_\Lambda$  ( $\Omega_\Lambda > \gamma$ ) the above inflection point exists.

In practice the condition  $\gamma < 1/3$  is amply satisfied in the context of RG-inspired models in which the vacuum energy evolves as in Eq. (22), the reason being that, in this QFT context,  $\gamma$  appears from Eq. (23) in which the highest scale  $M$  of the particle masses is expected to lie at (or below) the Planck scale. Therefore, from QFT we expect  $\gamma \ll 1$  and this is indeed what the comparison with experimental data confirms (see below). It is thus enlightening to expand (29) in the limit  $\gamma \ll 1$

$$a_I = \left( \frac{\Omega_m}{2\Omega_\Lambda} \right)^{1/3} \left\{ 1 - \gamma \left[ 1 + \frac{1}{3} \left( \ln \frac{2\Omega_\Lambda}{\Omega_m} - \frac{1}{\Omega_\Lambda} \right) \right] \right\}. \quad (30)$$

Since the coefficient  $\gamma$  in this formula is positive (for the current values of the cosmological parameters), we see that the transition point from deceleration to acceleration oc-

curs earlier in time than in the concordance  $\Lambda$ CDM model (20), whereas for  $\gamma < 0$  it occurs at a more recent time.

Let us also consider the behavior of the matter and vacuum energy densities in this model as a function of the scale factor. Starting from the conservation law [see Eq. (3)], and then trading the time derivatives for derivatives with respect to the scale factor, we obtain

$$\frac{d\rho_m}{da} + \frac{3}{a}\rho_m = -\frac{d\Lambda}{da}. \quad (31)$$

Using this equation in combination with (3) and (22), we arrive at a simple differential equation for the matter density,

$$\frac{d\rho_m}{da} + \frac{3}{a}(1 - \gamma)\rho_m = 0, \quad (32)$$

whose trivial integration yields

$$\rho_m(a) = \rho_{m0}a^{-3(1-\gamma)}. \quad (33)$$

Here  $\rho_{m0}$  is the matter density at the present time ( $a = 1$ ). Similarly, we find

$$\Lambda(a) = \Lambda_0 + \frac{\gamma\rho_{m0}}{1-\gamma}[a^{-3(1-\gamma)} - 1]. \quad (34)$$

Substituting Eq. (25) in the last two equations one may obtain the explicit time evolution of the matter and vacuum energy densities, if desired. It is important to emphasize from Eq. (33) that the matter density does no longer evolve as  $\rho_m(a) = \rho_{m0}a^{-3}$ , as it presents a correction in the exponent. This is due to the fact that matter is exchanging energy with the vacuum and this is reflected in the corresponding behavior of  $\Lambda(a)$  in Eq. (34). Substituting Eq. (34) in Eq. (22), we immediately obtain

$$\begin{aligned} E^2(a) &= \frac{\Omega_\Lambda - \gamma}{1 - \gamma} + \frac{\Omega_m}{1 - \gamma}a^{-3(1-\gamma)} \\ &= 1 + \Omega_m \frac{a^{-3(1-\gamma)} - 1}{1 - \gamma}, \end{aligned} \quad (35)$$

where in the second step we have used the cosmic sum rule for flat space  $\Omega_m + \Omega_\Lambda = 1$ . Needless to say, Eq. (35) can also be obtained by eliminating the cosmic time from Eqs. (24) and (25), as one can check. It is worth noting that the normalized Hubble flow in this model [see Eq. (35)] can be viewed in a similar formulation as that of the concordance cosmology (for more details see Appendix A) as follows:

$$E^2(a) = \tilde{\Omega}_\Lambda + \tilde{\Omega}_m a^{-3(1-\gamma)}, \quad (36)$$

where

$$\tilde{\Omega}_m = 1 - \tilde{\Omega}_\Lambda = \frac{\Omega_m}{1 - \gamma}. \quad (37)$$

As expected, for  $\gamma \rightarrow 0$  ( $\tilde{\Omega}_m \sim \Omega_m$ ) all the above equations boil down to the canonical form within the concord-

ance model—cf. previous section. Thus, the traditional  $\Lambda$  cosmology is a particular solution of the  $\Lambda_{\text{RG}}$  model with  $\gamma$  strictly equal to 0.

Comparing the  $\Lambda_{\text{RG}}$  model with the observational data (we sample  $\gamma \in [-1, 0.3]$  in steps of 0.001) we find that the best fit value is  $\Omega_m = 0.28^{+0.02}_{-0.01}$  (or  $\tilde{\Omega}_m \simeq 0.281$ ) and  $\gamma = 0.002 \pm 0.001$  with  $\chi^2_{\text{tot}}(\Omega_m, \gamma) \simeq 431.2$  for dof = 351. We remark that the best fit value that we have obtained for  $\gamma$  using the combined set of modern SNIa + BAO + CMB data becomes significantly smaller than the one obtained in the old analysis of Ref. [32], where only a limited set of 54 supernovae data was employed.<sup>1</sup> In fact, here we have been able to further restrict the parameter  $\gamma$  (called  $\nu$  in [32]) and push its value to its natural small range (viz.  $\gamma \sim 10^{-3}$  or below) as expected from general QFT considerations [36]—see Eq. (23).

Being  $\gamma$  small and positive, Eq. (30) predicts that the transition point from deceleration to acceleration should be slightly earlier in time (hence at larger redshift) as compared to the standard  $\Lambda$ CDM case.

It is interesting to point out that the small  $\gamma$  value that we have obtained from the combined SNIa + BAO + CMB data is nicely compatible with the result obtained for this parameter from the analysis of the matter power spectrum of that model, performed in [60]—see also [61]. Here we will analyze also the linear perturbation regime for the various models. However, rather than focusing on the power spectrum we will test the implications of this model on structure formation, through the study of the growth rate  $d \ln D(a)/d \ln a$ , the formation of galaxy clusters and the evolution of their abundances (see Secs. V and VI). In all cases we need to find the linear matter fluctuation field  $D(a)$ , which we shall determine under the assumption of vanishing  $\Lambda$  perturbations. As we have explained in Sec. II, this is justified for perturbations well inside the sound horizon and assuming that the produced matter particles have negligible velocities with respect to the comoving observers.

Therefore, we now proceed in an attempt to analytically solve the differential Eq. (5) in order to investigate the matter fluctuation field of the RG model (22) in the linear regime. To do so, we change variables from  $t$  to a new one according to the transformation

$$y = \coth \left[ \frac{3}{2} H_0 \sqrt{(\Omega_\Lambda - \gamma)(1 - \gamma)} t \right]. \quad (38)$$

Also from Eqs. (24), (25), and (35), we get the following useful relations:

$$y = \sqrt{\frac{\beta}{\Omega_\Lambda - \gamma}} E(a), \quad y^2 - 1 = \frac{\Omega_m}{\Omega_\Lambda - \gamma} a^{-3\beta}, \quad (39)$$

where  $\beta \equiv 1 - \gamma$ . Using (38) and (39) we find, after some

<sup>1</sup>However, using the current SNIa data alone our best fit values are in agreement with those found by [32].

algebra, that Eq. (5) takes on the form

$$3\beta^2(y^2 - 1)^2 D'' + f(\beta)y(y^2 - 1)D' - 2[g(\beta)y^2 - \psi(\beta)]D = 0, \quad (40)$$

where primes denote derivatives with respect to  $y$ , and

$$f(\beta) = 2\beta(6\beta - 5), \quad g(\beta) = (2 - \beta)(3\beta - 2), \\ \psi(\beta) = \beta(4 - 3\beta). \quad (41)$$

In deriving Eq. (40) we have substituted the various terms in (5) as a function of the new variable [see Eq. (39)] and the cosmological parameters. For instance, from Eqs. (6), (22), (33), and (39), we have

$$\rho_m = 3H_0^2(\Omega_\Lambda - \gamma)(y^2 - 1) \quad Q = 3\gamma H_0 \sqrt{\frac{\Omega_\Lambda - \gamma}{1 - \gamma}} y \\ \dot{Q} = \frac{9}{2} \gamma H_0^2 (\Omega_\Lambda - \gamma) (1 - y^2). \quad (42)$$

Factors of  $H_0$  drop at the end of the calculation. The differential Eq. (40) can be brought into the standard associated Legendre form by an appropriate transformation. The growth factor solving this equation reads

$$D(y) = \mathcal{C}(y^2 - 1)^{4-9\beta/6\beta} y F\left(\frac{1}{3\beta} + \frac{1}{2}, \frac{3}{2}, \frac{1}{3\beta} + \frac{3}{2}, -\frac{1}{y^2 - 1}\right) \quad (43)$$

where the quantity  $F$  is the hypergeometric function and  $\mathcal{C}$  is a constant (for more details see Appendix B). Inserting Eq. (39) into Eq. (43) and using (37), we finally obtain the growth factor  $D(a)$  as a function of the scale parameter

$$D(a) = C_1 a^{9\beta-4/2} E(a) F\left(\frac{1}{3\beta} + \frac{1}{2}, \frac{3}{2}, \frac{1}{3\beta} + \frac{3}{2}, -\frac{\tilde{\Omega}_\Lambda}{\tilde{\Omega}_m} a^{3\beta}\right) \quad (44)$$

where

$$C_1 = \mathcal{C} \tilde{\Omega}_\Lambda^{-1} \left(\frac{\tilde{\Omega}_m}{\tilde{\Omega}_\Lambda}\right)^{(4-9\beta)/6\beta}. \quad (45)$$

As a consistency check we note that for  $\gamma = 0$  ( $\beta = 1$ ), the corresponding normalized to unity growth factor derived from Eq. (44) provides the same results as those of the concordance cosmology [see Eq. (21)]. From this analysis, it becomes clear that the overall dynamics, predicted by the  $\Lambda_{\text{RG}}$  model, extends nicely to that of the usual  $\Lambda$  cosmology and connects smoothly to it. For the analysis of other RG-inspired phenomenological time varying  $\Lambda$  models, see [62].

### C. The $\Lambda(t) \propto H^2$ model

We now consider that the vacuum energy density decays as:  $\Lambda = 3\gamma H^2$  (hereafter  $\Lambda_{H_1}$ —see [29,40]). This model

corresponds in setting  $n_0 = 0$  in Eq. (15), and therefore it can be derived as a particular case of the previous model. In this context, the basic cosmological equations become

$$H(t) = \frac{2}{3(1-\gamma)t}, \quad a(t) = \left[\frac{3(1-\gamma)}{2} H_0 t\right]^{2/3(1-\gamma)} \quad (46)$$

and the normalized Hubble flow is

$$E(a) = a^{-3(1-\gamma)/2}. \quad (47)$$

Note, that the constant  $\gamma$  lies in the interval  $0 \leq \gamma < 1$ , while the vacuum energy density remains constant everywhere, which implies that  $\Omega_m(a) = 1 - \gamma$ . This is consistent with the cosmic sum rule, since  $\gamma = \Omega_\Lambda$  for this model. From Eq. (46) it is obvious that this model has no inflection point.

If we change the variables from  $t$  to  $a$  then the time evolution of the mass density contrast [see Eq. (5)] takes the following form:

$$a^2 D'' + \frac{3}{2} a(1 + 3\gamma) D' - \frac{3}{2} (1 + \gamma)(1 - 3\gamma) D = 0 \quad (48)$$

a general solution of which is

$$D(a) = C_1 a^{1-3\gamma} + C_2 a^{-3(1+\gamma)/2} \quad (49)$$

where  $C_1$  and  $C_2$  are the corresponding constants. Notice, that a growing mode is present in this scenario if and only if  $\gamma < 1/3$ , which implies that cosmic structures cannot be formed via gravitational instability in  $\Lambda_{H_1}$  models with  $\gamma \geq 1/3$ . From a theoretical viewpoint, it is obvious that the  $\Lambda_{H_1}$  pattern modifies the Einstein de Sitter model.

We find that the current model is unable to fit the combined observational data (SNIa + BAO + CMB). Indeed, we find that  $\gamma = 0.64_{-0.01}^{+0.02}$  with  $\chi^2_{\text{SNIa+BAO}} \simeq 459.3$ . Interestingly, the addition of one more point (the CMB shift parameter) increases the overall likelihood function by a factor of  $\sim 2.4$  [ $\chi^2_{\text{tot}}(\gamma) \simeq 1104.8$  with  $\gamma = 0.95 \pm 0.01$ ]. Using any of the fitted values of  $\gamma$ , it then follows from Eq. (46) that for this model the scale factor evolves as  $a \sim t^\epsilon$  with  $\epsilon > 1$ . Under these conditions, this model is free from the horizon problem. However, unfortunately, it is unable to fit the present observational data, and moreover combining the latter statistical result with the  $\gamma < 1/3$  constrain we conclude that the current cosmological model is ruled out at high significance level.

### D. A power series $\Lambda(t)$ model

In this case, we parametrize the functional form of  $\Lambda(t)$  using a power series expansion in  $H$  up to the second order (see [51]) and assuming that there is no constant term

$$\Lambda = n_1 H + n_2 H^2 \quad (50)$$

(hereafter  $\Lambda_{\text{PS}_1}$ ). Performing the integration of Eq. (4) we derive the following Hubble function:

$$H(t) = \frac{n_1}{\gamma} \frac{e^{n_1 t/2}}{e^{n_1 t/2} - 1}, \quad (51)$$

where we have defined  $\gamma = 3 - n_2$  and expect  $\gamma$  to remain around 3 (or  $|n_2| \ll 1$ ). In fact, we do not foresee that the coefficient  $n_2$  could be large (for similar reasons as in Sec. IV B). Using now that  $H \equiv \dot{a}/a$ , the scale factor of the universe  $a(t)$ , evolves with time as

$$a(t) = a_1 (e^{n_1 t/2} - 1)^{2/\gamma}, \quad (52)$$

where  $a_1$  is the constant of integration. From these equations, we can easily write the corresponding Hubble flow as a function of the scale factor

$$H(a) = \frac{n_1}{\gamma} \left[ 1 + \left( \frac{a}{a_1} \right)^{-\gamma/2} \right]. \quad (53)$$

Evaluating Eq. (53) at the present time ( $a \equiv 1$ ), we obtain

$$n_1 = \frac{\gamma H_0}{1 + a_1^{\gamma/2}}. \quad (54)$$

Now utilizing Eqs. (50) and (54) and taking into account that the current value of the vacuum energy density is  $\Lambda_0 = 3H_0^2 \Omega_\Lambda$  ( $\Omega_\Lambda = 1 - \Omega_m$ ), we arrive at

$$a_1 = \left( \frac{3\Omega_m}{\gamma - 3\Omega_m} \right)^{2/\gamma}, \quad n_1 = H_0(\gamma - 3\Omega_m). \quad (55)$$

Obviously, the above equation implies the following condition:  $\gamma > 3\Omega_m$  (or  $n_2 < 3\Omega_\Lambda$ ).

The normalized to unity, at the present epoch, scale factor of the universe becomes

$$a(t) = \left( \frac{3\Omega_m}{\gamma - 3\Omega_m} \right)^{2/\gamma} [e^{H_0(\gamma - 3\Omega_m)t/2} - 1]^{2/\gamma} \quad (56)$$

or

$$t(a) = \frac{2}{H_0(\gamma - 3\Omega_m)} \ln \left[ \frac{\gamma a^{\gamma/2} E(a)}{3\Omega_m} \right] \quad (57)$$

where

$$E(a) = \frac{H(a)}{H_0} = 1 - \frac{3\Omega_m}{\gamma} + \frac{3\Omega_m}{\gamma} a^{-\gamma/2}. \quad (58)$$

It is interesting to point here that the current age of the universe [ $a = 1$ ,  $E(1) = 1$ ] is

$$t_0 = \frac{2}{H_0(\gamma - 3\Omega_m)} \ln \left( \frac{\gamma}{3\Omega_m} \right). \quad (59)$$

We now study the conditions under which an inflection point exists in our past, implying an acceleration phase of the scale factor. This crucial period in the cosmic history corresponds to  $\ddot{a}(t_I) = 0$  and  $t_I < t_0$ . Differentiating twice Eq. (56), we simply have

$$a_I = \left[ \frac{3(\gamma - 2)\Omega_m}{2(\gamma - 3\Omega_m)} \right]^{2/\gamma}, \quad t_I = \frac{2}{H_0(\gamma - 3\Omega_m)} \ln \left( \frac{\gamma}{2} \right), \quad (60)$$

which implies that the condition for which an inflection point is present in our past is  $\gamma > 2$ .

Performing now our statistical analysis we attempt to put constrains on the free parameters. In particular, we sample  $\gamma \in [2, 5]$  in steps of 0.01. Thus, the overall likelihood function peaks at  $\Omega_m = 0.32_{-0.02}^{+0.01}$ ,  $\gamma = 3.44 \pm 0.02$  with  $\chi_{\text{tot}}^2(\Omega_m, \gamma) = 432.7$  (dof = 351). Using the latter cosmological parameters the corresponding current age of the universe is found to be  $t_0 \sim 14.3$  Gyr while the inflection point is located at  $(a_I, t_I) \simeq (0.48, 0.42t_0)$ . This corresponds to a redshift  $z_I \simeq 1.08$ , which is substantially higher than in the case of the concordance model.

Following the notations of [51], we now derive the growth factor of fluctuations in the power series model. In particular, we change variables from  $t$  to a new one following the transformation

$$y = \exp(n_1 t/2) \quad \text{with } 0 < y < 1. \quad (61)$$

In this context, using Eqs. (6), (50), (53), and (61), we obtain

$$\begin{aligned} \rho_m &= \frac{n_1^2 y}{\gamma(y-1)^2} & Q &= \frac{n_1[(6-\gamma)y - \gamma]}{2\gamma(y-1)} \\ \dot{Q} &= \frac{n_1^2(\gamma-3)y}{2\gamma(y-1)^2}, \end{aligned} \quad (62)$$

[for  $n_1$  see Eq. (55)].

We can now rewrite Eq. (5) as

$$\begin{aligned} \gamma^2 y(y-1)^2 D'' + 2\gamma(y-1)(5y-\gamma)D' \\ - 2(6-\gamma)(\gamma-2y)D = 0 \end{aligned} \quad (63)$$

where prime denotes derivatives with respect to  $y$ . Notice, that this variable is related with the scale factor as

$$y = 1 + \frac{\gamma - 3\Omega_m}{3\Omega_m} a^{\gamma/2}. \quad (64)$$

We find that Eq. (63) has a decaying solution of the form  $D_1(y) = (y-1)^{(\gamma-6)/\gamma} \sim a^{(\gamma-6)/2}$  for  $\gamma < 8$ . Thus, the corresponding growing mode of Eq. (63) is

$$D(a) = C a^{(\gamma-6)/2} \int_0^a \frac{dx}{x^{\gamma/2} E^2(x)} \quad (65)$$

where

$$C = \frac{\gamma}{2} \tilde{\Omega}_m^2 \left( \frac{\tilde{\Omega}_\Lambda}{\tilde{\Omega}_m} \right)^{(2\gamma-4)/\gamma} \quad (66)$$

with

$$\tilde{\Omega}_m = 1 - \tilde{\Omega}_\Lambda = \frac{3\Omega_m}{\gamma}. \quad (67)$$

It is interesting to mention that, the normalized Hubble flow [see Eq. (58) and Appendix A] can be cast as

$$E(a) = \tilde{\Omega}_\Lambda + \tilde{\Omega}_m a^{-\gamma/2}. \quad (68)$$

It becomes clear that for  $\gamma \rightarrow 3$  we have  $\Omega_m \sim \tilde{\Omega}_m$ . Using our best fit values we find  $\tilde{\Omega}_m \simeq 0.28$ . Finally, in the limit of  $n_1 \rightarrow 0$  (or  $n_2 \rightarrow 3\tilde{\gamma}$ ;  $\tilde{\gamma}$  is a constant) the current cosmological pattern tends to the  $\Lambda_{H_1}$  model (see Sec. IV C) as it should [ $\Lambda(a) \sim 3\tilde{\gamma}H^2$ ,  $E(a) \sim a^{-3(1-\tilde{\gamma})/2}$ , and  $D(a) \sim a^{1-3\tilde{\gamma}}$ ].

### E. The $\Lambda \propto H$ model

As we have previously mentioned, different authors [53–55,59] have tried to provide some fundamental reason for the possibility that the vacuum term could be proportional to the Hubble parameter,  $\Lambda(a) \propto H$ . Note, that this kind of cosmological model (hereafter  $\Lambda_{\text{PS}_2}$ ) is a particular case of the power series model studied in the previous section by setting  $n_2 = 0$  in Eq. (50):

$$\Lambda = n_1 H. \quad (69)$$

In this case, the normalized Hubble flow simply reads as in (68), but using the original (untilded) cosmological parameters and choosing  $\gamma = 3$ :

$$E(a) = \Omega_\Lambda + \Omega_m a^{-3/2}. \quad (70)$$

One of the merits of the  $\Lambda_{\text{PS}_2}$  vacuum model is that it contains only one free parameter,  $n_1$ . Obviously, this parameter is determined to be

$$n_1 = 3H_0\Omega_\Lambda. \quad (71)$$

Therefore, since we use the prior  $H_0 = 70.5$  km/sec/Mpc [3], the free parameter is actually  $\Omega_\Lambda$  (or, equivalently,  $\Omega_m = 1 - \Omega_\Lambda$ ). This single parameter is the same as in the standard flat  $\Lambda$ CDM model, except that the Hubble rate in (70), after squaring it, compares very differently with Eq. (19). Needless to say, this could make a dramatic difference when we try to fit the combined SNIa + BAO + CMB data with the  $\Lambda_{\text{PS}_2}$  model.

Indeed, if we now marginalize the results of the previous section over  $\gamma = 3$ , the joint likelihood analysis provides a best fit value of  $\Omega_m = 0.34 \pm 0.01$ , which is significantly larger than in the  $\Lambda$ CDM case, but with a poor quality fit:  $\chi_{\text{tot}}^2(\Omega_m) \simeq 513.6$  for dof = 352 [51].

This simply means that the functional form (70) is unable to fit the observational data simultaneously at low and high redshifts. We confirm this point by using only the CMB shift parameter in the  $\chi^2$  minimization, finding that the corresponding likelihood function peaks at  $\Omega_m \simeq 0.80$ . This value is  $\sim 2.5$  times larger than that provided by the SNIa + BAO solution,  $\Omega_m \simeq 0.32$ . This fact alone suggests that in spite of the various adduced motivations in the literature for the class of models  $\Lambda \propto H$ , they are

unfortunately unable to provide a quality fit of the basic cosmological data in all the relevant redshift ranges.

We note that although our combined SNIa + BAO + CMB likelihood analysis provides a similar  $\Omega_m$  value to that found in [49], it has a quite large reduced  $\chi^2$  ( $\simeq 1.46$ ), which is in contrast with Carneiro *et al.* who concluded that the  $\Lambda \propto H$  model was compatible with the data they used. However, this conclusion immediately paled after performing the study of the matter power spectrum of such model, which turned out to be highly unfavorable owing to a significant late-time depletion of power as compared to the standard  $\Lambda$ CDM model [50]. We find that this is borne out by the present study; in fact, the growth rate of galaxy clustering becomes frozen at late times for that model (as we will see in Sec. V). The analysis of the fluctuation field  $D(a)$  is performed exactly as in Sec. IV D in the limit  $\gamma \rightarrow 3$ .

### F. A power law $\Lambda(t)$ model

In this phenomenological scenario, we generalize the ideology of [28,47] in which the vacuum energy density evolves as  $\Lambda(a) \propto a^{-2}$ . In the present work, the vacuum energy is taken to evolve with an arbitrary power of the scale factor

$$\Lambda(a) = 3\gamma(3-n)a^{-n} \quad (72)$$

(hereafter  $\Lambda_n$  model; see also [63]). The corresponding Hubble flow as a function of the scale factor follows from solving Eq. (4) with  $\Lambda$  given as in Eq. (72). Trading the cosmic time variable for the scale factor, the differential Eq. (4) can be seen as

$$\frac{dH^2}{da} + \frac{3}{a}H^2 = 3\gamma(3-n)a^{-n-1}. \quad (73)$$

The corresponding solution satisfying the boundary condition  $H(a=1) = H_0$  reads as follows:

$$H^2(a) = (H_0^2 - 3\gamma)a^{-3} + 3\gamma a^{-n}. \quad (74)$$

Using now the following parametrization,

$$\tilde{\Omega}_\Lambda = 1 - \tilde{\Omega}_m = \frac{3\gamma}{H_0^2}, \quad (75)$$

we simply derive

$$E^2(a) = \tilde{\Omega}_m a^{-3} + \tilde{\Omega}_\Lambda a^{-n}. \quad (76)$$

Evidently, if we parametrize the constant  $n$  according to  $n = 3(1+w)$  then the current  $\Lambda_n$  cosmological model can be viewed as a classical *quintessence* model ( $P_Q = w\rho_Q$ ) with  $w < -1/3$  (or  $n < 2$ ), as far as the global dynamics is concerned [63]), despite the fact that the two models have a different equation of state parameter. On the other hand, utilizing Eq. (72) at the present epoch [ $\Lambda_0 = 3\gamma(3-n)$ ] and taking into account that the current value of the vacuum energy density is  $\Lambda_0 = 3H_0^2\Omega_\Lambda$  we obtain

$$\gamma = \frac{\Omega_\Lambda H_0^2}{3-n}, \quad (77)$$

and

$$\tilde{\Omega}_\Lambda = 1 - \tilde{\Omega}_m = \frac{3\Omega_\Lambda}{3-n}. \quad (78)$$

Obviously, for  $n \rightarrow 0$  we get  $\tilde{\Omega}_\Lambda \sim \Omega_\Lambda$  (or  $\tilde{\Omega}_m \sim \Omega_m$ ) as we should.

It is worthwhile to compute the evolution of the matter density as a function of the scale factor. From (1), (72), and (74) we find

$$\rho_m(a) = 3(H_0^2 - 3\gamma)a^{-3} + 3n\gamma a^{-n}. \quad (79)$$

We remark that, in spite of the simple form of the Hubble rate (76) in terms of the formal parameters ( $\tilde{\Omega}_m, \tilde{\Omega}_\Lambda$ ) (see Appendix A), the matter density is a mixture of the canonical  $a^{-3}$  component and the new  $a^{-n}$  component associated to the vacuum energy. This was expected from the fact that matter and vacuum energy are in interaction in this model. The physical parameters ( $\Omega_m, \Omega_\Lambda$ ) are related in the standard manner. Indeed, since  $\rho_{m0} = \rho_m(a=1)$ , we have from (79)

$$\Omega_m = \frac{\rho_{m0}}{3H_0^2} = 1 - \frac{\gamma(3-n)}{H_0^2} = 1 - \Omega_\Lambda, \quad (80)$$

which is consistent with the result found above for  $\Omega_\Lambda$ .

Comparing the  $\Lambda_n$  model with the observational data (we sample  $n \in [-0.2, 2]$  in steps of 0.01) we find that the best fit values are  $\Omega_m = 0.29_{-0.02}^{+0.01}$  (or  $\tilde{\Omega}_m \simeq 0.28$ ) and  $n = -0.06 \pm 0.04$  with  $\chi_{\text{tot}}^2(\Omega_m, n) \simeq 431.2$  (dof = 351). The standard  $\Lambda$ CDM case is obtained from this model for  $n = 0$ , and the best fit value is indeed close to it, but the fact that  $n$  approaches 0 from below (implying  $w \simeq -1.02$ ) means that the preferred situation is slightly tilted into the phantom domain. The inflection point for this model can be easily computed without resorting to the time dependence as follows. Requiring that the deceleration parameter

$$q = -\frac{\ddot{a}a}{\dot{a}^2} = -1 - \frac{a}{2H^2(a)} \frac{dH^2}{da} \quad (81)$$

vanishes, we find that  $adH^2/da + 2H^2 = 0$ , and hence  $a_I$  is the root of this equation. Using (74) and (77), we are immediately led to

$$a_I = \left[ \frac{3\Omega_m - n}{3(2-n)\Omega_\Lambda} \right]^{1/(3-n)}, \quad (82)$$

which implies that  $n < 2$  for  $\Omega_m \in (0, 1)$ . Using our best fit values, we find  $a_I \simeq 0.60$  ( $z_I \simeq 0.66$ ), while the age of the universe is  $t_0 \sim 13.6$  Gyr. We remark that, contrary to the previous models, the power law model predicts a transition point from deceleration to acceleration located at a time more recent than the concordance model.

Finally, if we change the variables from  $t$  to  $a$  then the evolution of the mass density contrast [see Eq. (5)] be-

comes

$$a^2 H^2 D'' + a[3H^2 + aHH' + HQ]D' - G(a)D = 0 \quad (83)$$

where

$$G(a) = \frac{\rho_m}{2} - 2HQ - aHQ'. \quad (84)$$

Because of the fact that the best fit value  $n = -0.06$  is relatively small, we can neglect from Eq. (83) the corresponding high order terms ( $n^2, n^3, n\Omega_m\Omega_\Lambda$ , etc). Thus, we obtain the following accurate formula to the growth factor (see also [63])

$$D(a) \simeq aF\left(-\frac{1}{3w}, \frac{w-1}{2w}, 1 - \frac{5}{6w}, -\frac{\tilde{\Omega}_\Lambda a^{-3w}}{\tilde{\Omega}_m}\right) \quad (85)$$

where  $w = -1 + n/3$  and  $F$  is the hypergeometric function. Notice that  $D(a) \sim a$  for  $\Omega_\Lambda \rightarrow 0$ , as expected.

## V. LINEAR GROWTH RATE FOR THE TIME VARYING VACUUM MODELS

In the upper panel of Fig. 1 we present the growth factor evolution, for the different time varying vacuum models, presented in this work, as a function of redshift,  $D(z)$  [ $z = a^{-1} - 1$ ]. Notice, that the growth factors are normalized to unity at the present time ( $z = 0$ ). We find that for  $z \leq 0.5$  the  $\Lambda_{\text{PS}_1}$  and  $\Lambda_{\text{PS}_2}$  growth factors reach a plateau, implying that the matter fluctuations are effectively frozen, as we already advanced in Sec. IV E. Also, it is obvious that the growth factors for the latter vacuum models are much greater with respect to the other 3 models,  $\Lambda$ ,  $\Lambda_{\text{RG}}$ , and  $\Lambda_n$ . Therefore, it is expected that this difference among the above cosmological models will affect also the predictions related with the formation of the cosmic structures (see next section), due to the fact that they trace differently the evolution of the matter fluctuation field.

We would like to end this section with a discussion on the evolution of the well-known indicator of clustering, namely, the growth rate [57]

$$f(a) \equiv \frac{d \ln D}{d \ln a}. \quad (86)$$

From the known analytical form of the growth factor  $D(a)$  for the current vacuum models,<sup>2</sup> in the bottom panel of Fig. 1 we display the predicted growth rate

$$f(z) = -(1+z) \frac{d \ln D}{dz}, \quad (87)$$

together with the observed  $f_{\text{obs}}(z)$  [filled symbols] using the recent results of the 2dF and SDSS galaxies [64]. In

<sup>2</sup>The formula  $\frac{d}{dx} F(a, b, c, x) = \frac{ab}{c} F(a+1, b+1, c+1, x)$  after differentiating the hypergeometric function is used to compute  $f(z)$  from  $D(z)$ .

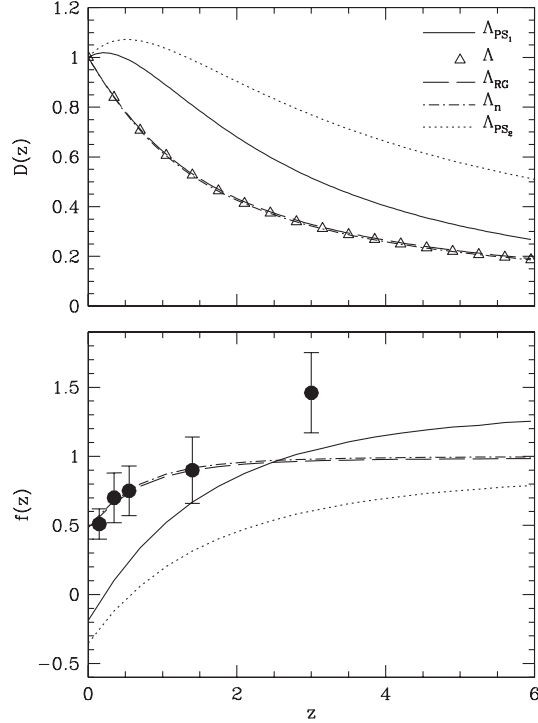


FIG. 1. Upper Panel shows the evolution of the growth factor. The lines correspond to  $\Lambda_{\text{PS}_1}$  (solid),  $\Lambda_{\text{RG}}$  (dashed),  $\Lambda_n$  (dot-dashed), and  $\Lambda_{\text{PS}_2}$  (dot). Note, that open triangles correspond to the traditional  $\Lambda$  cosmology. Bottom Panel: shows a comparison of the observed (solid circles) [64], (see Table I) and theoretical evolution of the growth rate of clustering  $f(z)$ . We do not plot the growth rate of the  $\Lambda$  cosmology in order to avoid confusion.

Table I, we quote the precise numerical values of the data points, with the corresponding error bars. We compare the growth rate of clustering between data and models via a  $\chi^2$  minimization and a Kolmogorov-Smirnov (KS) statistical test, respectively. For the model predictions we use the best fitted value for the parameters ( $\gamma$  or  $n$ ) obtained in Sec. IV for each model. We then compute the corresponding consistency between models and data ( $\chi^2_{\text{min}}/5$  and  $\mathcal{P}_{\text{KS}}$ ) and place these results in Table II. Obviously, in the case of  $\Lambda$ ,  $\Lambda_{\text{RG}}$ , and  $\Lambda_n$  models we find good consistency ( $\chi^2_{\text{min}}/5 \approx 0.64$  and  $\mathcal{P}_{\text{KS}} \approx 1$ ). Therefore, it is apparent that the power series  $\Lambda_{\text{PS}_1}$  and  $\Lambda_{\text{PS}_2}$  vacuum models (and especially the

TABLE I. Data of the growth rate of clustering [64]. The correspondence of the columns is as follows: redshift, observed growth rate, and references.

$z$	$f_{\text{obs}}$	Refs.
0.15	$0.51 \pm 0.11$	[65,66]
0.35	$0.70 \pm 0.18$	[67]
0.55	$0.75 \pm 0.18$	[68]
1.40	$0.90 \pm 0.24$	[69]
3.00	$1.46 \pm 0.29$	[70]

TABLE II. The reduced  $\chi^2$  values ( $\chi^2_{\text{min}}/df$ ) and KS probabilities comparing the growth rate of clustering between data and vacuum model expectations.

Model	$\chi^2_{\text{min}}/5$	$\mathcal{P}_{\text{KS}}$	$\chi^2_{\text{min}}/4(z < 3)$	$\mathcal{P}_{\text{KS}}(z < 3)$
$\Lambda$	0.63	1.0	0.10	0.997
$\Lambda_{\text{RG}}$	0.64	1.0	0.10	0.997
$\Lambda_{\text{PS}_1}$	9.7	0.210	11.6	0.107
$\Lambda_{\text{PS}_2}$	20	0.036	22.9	0.011
$\Lambda_n$	0.63	1.0	0.10	0.997

latter, which is the model where  $\Lambda$  evolves linearly with  $H$ ) fail to fit the data ( $\chi^2_{\text{min}}/5 \approx 20$  and  $\mathcal{P}_{\text{KS}} \approx 0.036$  for  $\Lambda_{\text{PS}_2}$ ). In this framework, close to the present epoch  $z \leq 0.5$ , the  $\Lambda_{\text{PS}_1}$  vacuum model is unable to fit the data ( $\chi^2_{\text{min}}/5 \approx 9.7$  and  $\mathcal{P}_{\text{KS}} \approx 0.21$ ) because the matter fluctuation field is frozen and thus the growth rate of clustering effectively overs. However, increasing the free parameter  $\gamma$  by a factor of  $\sim 1.2$  ( $\gamma \approx 4.1$ ) the  $\Lambda_{\text{PS}_1}$  model appears to fit the  $f_{\text{obs}}(z)$  data ( $\chi^2_{\text{min}}/5 \approx 1.2$  and  $\mathcal{P}_{\text{KS}} \approx 0.99$ ). Note, that in the last two rows of Table II, we list the corresponding results by excluding from the statistical analysis the observed growth rate of clustering at  $z = 3$  (see Table I [70]).

## VI. THE FORMATION AND EVOLUTION OF COLLAPSED STRUCTURES

In this section we study the cluster formation processes by using the usual Press-Schechter formalism [71], which studies the behavior of the matter perturbations assuming a Gaussian random field background, but applied also within the framework of the vacuum models studied in this work.

We wish here to estimate, within the different vacuum models, the fractional rate of cluster formation (see [72,73]). In particular, these studies introduce a methodology which computes the rate at which mass joins virialized halos (such as galaxy clusters), which grow from small initial perturbations in the universe, with matter fluctuations,  $\delta$ , greater than a critical value  $\delta_c$ .

Assuming that the density fluctuation field, smoothed at the scale  $R$  (corresponding to a mass scale of  $M = 4\pi\bar{\rho}R^3/3$ , with  $\bar{\rho}$  the mean background mass density of the Universe), is normally distributed with zero mean, then the probability that the field will have a value  $\delta$  at any given point in space is

$$\mathcal{P}(\delta, z) = \frac{1}{\sqrt{2\pi}\sigma(R, z)} \exp\left[-\frac{\delta^2}{2\sigma^2(R, z)}\right], \quad (88)$$

where the variance of the Gaussian field,  $\sigma^2(R, z)$ , is given by

$$\sigma^2(R, z) = \frac{1}{2\pi^2} \int_0^\infty k^2 P(k, z) W^2(kR) dk \quad (89)$$

with  $P(k, z)$  the power spectrum of density fluctuations which evolves according to  $P(k, z) = P(k, 0)D^2(z)$ , with

$D(z)$  the growing mode of the density fluctuations evolution, normalized such that  $D(0) = 1$ . Finally,  $W(kR)$  is the top-hat smoothing kernel, given in Fourier-space by

$$W(kR) = \frac{3}{(kR)^3} [\sin(kR) - kR \cos(kR)]. \quad (90)$$

We can now estimate what fraction of the Universe, at some reference redshift  $z$  and above some mass threshold  $M$ , has collapsed to form bound structures. To this end we need to integrate the probability function given by Eq. (88) over all regions that at some prior redshift had overdensities which by the reference redshift have increased to above the critical value,  $\delta_c(z)$ , which in an Einstein-de Sitter universe is  $\simeq 1.686$  and varies slightly for different values of  $\Omega_m$  [74]. Therefore, this fraction is given by [73]

$$\mathcal{F}(M, z) = \int_{\delta_c(z)}^{\infty} \mathcal{P}(\delta, z) d\delta, \quad (91)$$

and performing the above integration, parametrizing the rms mass fluctuation amplitude at  $R = 8h^{-1}$  Mpc, which can be expressed as a function of redshift as  $\sigma(M, z) = \sigma_8(z) = D(z)\sigma_8$ , we obtain

$$\mathcal{F}(z) = \frac{1}{2} \left[ 1 - \operatorname{erf} \left( \frac{\delta_c}{\sqrt{2}\sigma_8(z)} \right) \right]. \quad (92)$$

Obviously the above generic form of Eq. (92) depends on the choice of the background cosmology and the power-spectrum normalization, which we take to be the WMAP5 result of  $\sigma_8 \simeq 0.80$  [3].

The final step is to normalize the above probability to give the fraction of mass in bound structures which have already collapsed by the epoch  $z$ , divided by the corresponding fraction in structures which have collapsed at the present epoch ( $z = 0$ ),

$$\tilde{\mathcal{F}}(z) = \mathcal{F}(z)/\mathcal{F}(0). \quad (93)$$

In Fig. 2 we present in a logarithmic scale the behavior of

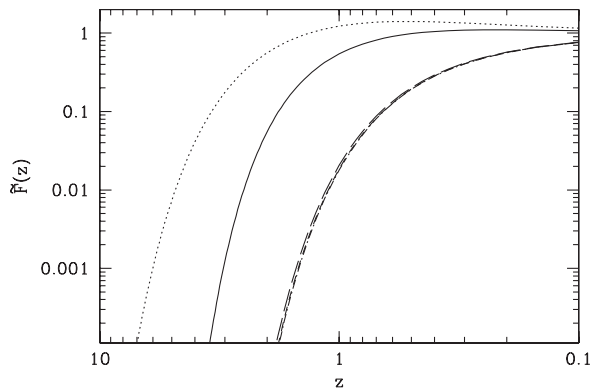


FIG. 2. The predicted fractional rate of cluster formation as a function of redshift for the current cosmological models (using  $\sigma_8 = 0.80$ ). The meaning of the various lines is as in Fig. 1.

normalized structure formation rate as a function of redshift for the present vacuum models.

In the context of the power series vacuum energy models (see  $\Lambda_{\text{PS}_1}$  solid line and  $\Lambda_{\text{PS}_2}$  dot line in Fig. 2), we find that prior to  $z \sim 0.5$  the cluster formation has effectively terminated due to the fact that the matter fluctuation field,  $D(z)$ , effectively freezes. Also, the large amplitude of the  $\Lambda_{\text{PS}_1}$  and  $\Lambda_{\text{PS}_2}$  fluctuation field (Fig. 1) implies that in these models galaxy clusters appear to form earlier ( $z \geq 4$ ) with respect to the  $\Lambda$ ,  $\Lambda_{\text{RG}}$ , and  $\Lambda_n$  (dashed lines) vacuum models. Indeed, for the latter cosmological models we find that galaxy clusters formed typically at  $z \sim 2$ . Finally, it is worth noticing that for a higher value of  $\sigma_8 (> 0.80)$ , the corresponding cluster formation rate moves to higher redshifts and obviously, the opposite situation is true for  $\sigma_8 < 0.80$ .

### The halo abundance and its evolution

From the previously presented Press-Schechter formalism (hereafter PSc), using the fraction of the universe,  $\mathcal{F}(M, z)$ , that has collapsed by some redshift in halos above some mass  $M$ , we can estimate the number density of halos,  $n(M, z)$ , with masses with a range  $(M, M + \delta M)$ , by the following:

$$n(M, z) dM = \frac{\partial \mathcal{F}(M, z)}{\partial M} \frac{\bar{\rho}}{M} dM. \quad (94)$$

Performing the differentiation and after some algebra we derive the following:

$$\begin{aligned} n(M, z) dM &= -\frac{\bar{\rho}}{M} \left( \frac{1}{\sigma} \frac{d\sigma}{dM} \right) f_{\text{PSc}}(\sigma) dM \\ &= \frac{\bar{\rho}}{M} \frac{d \ln \sigma^{-1}}{dM} f_{\text{PSc}}(\sigma) dM \end{aligned} \quad (95)$$

where  $f_{\text{PSc}}(\sigma) = \sqrt{2/\pi} (\delta_c/\sigma) \exp(-\delta_c^2/2\sigma^2)$ . Note that within this approach all the mass is locked inside halos, according to the normalization constraint

$$\int_{-\infty}^{+\infty} f_{\text{PSc}}(\sigma) d \ln \sigma^{-1} = 1. \quad (96)$$

Although the above (Press-Schechter) formulation was shown to give a good rough approximation to the expectations provided by numerical simulations, it was later found to overpredict or underpredict the number of low or high mass halos at the present epoch (eg. [75] and references therein). There is a large number of works providing better fitting functions of  $f(\sigma)$ , which are mostly based on a phenomenological approach (see [76] and references therein).

From the halo mass function we can now derive an observable quantity which is the redshift distribution of clusters,  $\mathcal{N}(z)$ , within some determined mass range, say  $M_1 \leq M/M_\odot \leq M_2$ . This can be estimated by integrating, in mass, the expected differential halo mass function,

$n(M, z)$ , according to

$$\mathcal{N}(z) = \frac{dV}{dz} \int_{M_1}^{M_2} n(M, z) dM \quad (97)$$

where  $dV/dz$  is the comoving volume element, which in a flat universe takes the form:

$$\frac{dV}{dz} = 4\pi r^2(z) \frac{dr}{dz}(z) \quad (98)$$

with  $r(z)$  the comoving radial distance out to redshift  $z$

$$r(z) = \frac{c}{H_0} \int_0^z \frac{dx}{E(x)}. \quad (99)$$

We use the halo mass function of Reed *et al.* [76], integrating for cluster-size halo masses, ie, between:  $10^{13.4} < M/M_\odot < 10^{16}$ . In Fig. 3 we show the integral halo mass function,  $n(>M)$ , for the models discussed previously and at two different redshifts. We use the WMAP5 normalization of the power spectrum, ie,  $\sigma_8 \simeq 0.8$ . Note that the classical  $\Lambda$ , the  $\Lambda_{\text{RG}}$ , and  $\Lambda_n$  models provide indistinguishable halo mass functions, with those corresponding to the  $\Lambda_{\text{PS2}}$  and  $\Lambda_{\text{PS1}}$  models being way off (we plot results only of the former model).

In Fig. 4 we show theoretically expected cluster redshift distribution for the three closely resembling models, ie, the standard  $\Lambda$  model, the  $\Lambda_{\text{RG}}$  and  $\Lambda_n$  models (left panel), and the fractional difference between the first (constant  $\Lambda$ ) and each of the other two models (right panel). The expected differences are small at low redshifts, but become gradually larger for  $z \gtrsim 2$ , reaching variations of up to  $\sim 100\%$  at  $z \sim 5$ . To investigate how realistic it would be to detect such differences, we provide below the expectations for two realistic cluster surveys covering the hole sky (although a more realistic case would be to consider a solid angle of the order of  $\sim 4 \times 10^3$  square degrees):

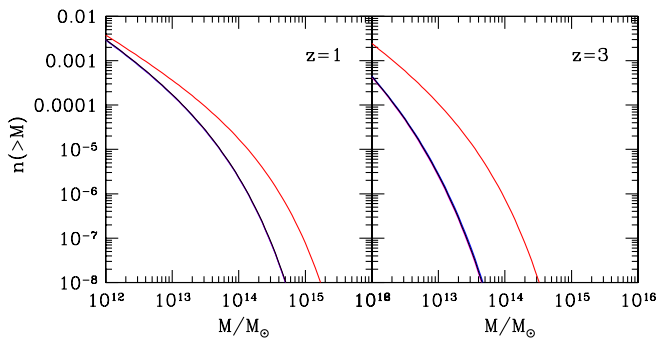


FIG. 3 (color online). The halo mass function at two different redshifts. The different models are represented by the same line-types as in the previous figures (which however fall on each other and thus are indistinguishable), but only the  $\Lambda_{\text{PS2}}$  model (upper curve) provides a significantly different  $n(M, z)$  than the other models.

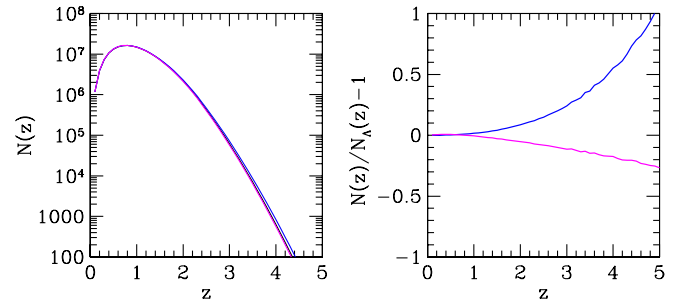


FIG. 4 (color online). The expected cluster redshift distribution (left panel) and the corresponding fractional difference (right panel) of the  $\Lambda_{\text{RG}}$  (upper blue curve) and  $\Lambda_n$  (lower magenta curve) models with respect to the standard  $\Lambda$  model.

- an X-ray survey down to a flux of:  $f_{\text{lim}} = 3 \times 10^{-14}$  ergs  $\text{s}^{-1} \text{cm}^{-2}$ , as that expected from the future eROSITA x-ray satellite, and
- a Sunayev-Zeldovich (SZ) survey with a limiting flux density at  $\nu_0 = 150$  GHz of  $f_{\nu_0, \text{lim}} = 5$  mJy (as expected from the survey of the Southern Polar Telescope).

To realize the predictions of the first survey we use the relation between halo mass and bolometric x-ray luminosity, as a function of redshift, provided in [77], ie

$$L(M, z) = 3.087 \times 10^{44} \left[ \frac{M_h h E(z)}{10^{15} M_\odot} \right]^{1.554} h^{-2} \text{ergs}^{-1}. \quad (100)$$

The limiting halo mass that can be observed at redshift  $z$  is then found by inserting in the above equation the limiting luminosity, given by  $L = 4\pi d_L^2 f_{\text{lim}}$ , with  $d_L$  the luminosity distance corresponding to the redshift  $z$ .

The predictions of the second survey can be realized using again the relation between limiting flux and halo mass from [77]

$$f_{\nu_0, \text{lim}} = \frac{2.592 \times 10^8 \text{ mJy}}{d_A^2(z)} \left( \frac{M}{10^{15} M_\odot} \right)^{1.876} E^{2/3}(z) \quad (101)$$

where  $d_A(z) \equiv d_L/(1+z)^2$  is the angular diameter distance out to redshift  $z$ .

In Fig. 5 we present the expected redshift distribution and the fractional difference between the different models, similarly to Fig. 4, but now for the realistic case of the x-ray survey. Similarly, in Fig. 6 we present the corresponding results for the case of the SZ survey. It is evident that the imposed flux-limit together with the scarcity of high-mass halos at large redshifts, induces an abrupt decline of the  $\mathcal{N}(z)$  with  $z$ , especially in the case of the cluster x-ray survey. As can be seen from the left panel of Fig. 5, this fact cancels the possibility of observing the intrinsic halo number-count differences between the different models ( $\Lambda$ ,  $\Lambda_{\text{RG}}$ , and  $\Lambda_n$ ). However, the expected SZ cluster number-counts (Fig. 6) show that we maybe able to detect significant differences in the redshift range  $2.5 \lesssim z \lesssim 3$  (at

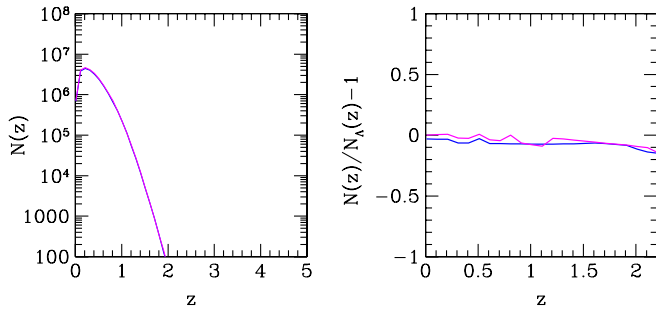


FIG. 5 (color online). The expected cluster redshift distribution (left panel) and the corresponding fractional difference (right panel) of the  $\Lambda_{\text{RG}}$  and  $\Lambda_n$  models with respect to the standard  $\Lambda$  model for the case of a realistic (future) x-ray survey with a flux limit of  $10^{-14}$  erg s $^{-1}$  cm $^{-2}$ .

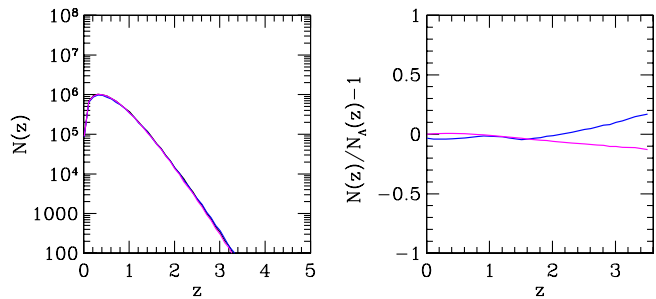


FIG. 6 (color online). The expected cluster redshift distribution (left panel) and the corresponding fractional difference (right panel) of the  $\Lambda_{\text{RG}}$  (upper blue curve) and  $\Lambda_n$  (lower magenta curve) models with respect to the standard  $\Lambda$  model for the case of a realistic (future) SZ survey with a flux limit of 5 mJy.

higher redshifts only a very small number of SZ clusters will be detected) at a level of  $\sim 6$ – $12\%$ , which translates in number-count differences, over the whole sky, of  $\sim 100$  clusters.

## VII. CONCLUSIONS

In this paper, we have studied analytically and numerically the overall dynamics of several time varying vacuum scenarios for spatially flat FLRW geometry, beyond the usual constant vacuum model (the standard  $\Lambda$ CDM cosmology). We wish to spell out clearly which are the basic assumptions and conclusions of our analysis.

- (i) We use various functional forms in order to parametrize the vacuum energy density. In particular, we consider: (a) a vacuum model based on the renormalization group (RG) in quantum field theory,  $\Lambda_{\text{RG}} = n_0 + n_2 H^2$ ; (b) a vacuum model in which  $\Lambda$  evolves proportional to the total energy density of the universe, hence  $\Lambda_{H_1} \propto H^2$ ; (c) a power series expansion in  $H$  up to the second order without constant term,  $\Lambda_{\text{PS}_1} = n_1 H + n_2 H^2$ ; (d) a vacuum energy density which decays proportional to the

Hubble expansion rate as  $\Lambda_{\text{PS}_2} = n_1 H$ ; and (e) a vacuum energy density which evolves with an arbitrary power of the scale factor as  $\Lambda_n = 3\gamma(3 - n)a^{-n}$ . These models have different theoretical motivations, but not all of them are able to withstand the stringent experimental tests provided by the various observational sources. In this framework, we first perform a joint likelihood analysis in order to put tight constraints on the main cosmological parameters by using the current observational data (SNIa, BAOs, and CMB shift parameter, together with the growth rate of galaxy clustering). Also, we find that the above models can accommodate a late time accelerated expansion.

- (ii) In the case of the power series models  $\Lambda_{\text{PS}_1}$  and  $\Lambda_{\text{PS}_2}$ , we find that the amplitude and the shape of the linear density contrast are for both significantly different with respect to those of the  $\Lambda$ ,  $\Lambda_{\text{RG}}$ , and  $\Lambda_n$  models. We also find that for  $z \leq 0.5$  the matter fluctuation field of the power series models practically freezes out, which indicates that the corresponding growth rate of clustering tends to zero. The latter result is ruled out by the observed growth rate of clustering measured from the optical galaxies. In the particular case of  $\Lambda_{\text{PS}_2}$ , even the fit of the cosmological parameters turns out to be of poor quality because it is unable to adjust simultaneously the observational data at low and high redshift. In contrast, the  $\Lambda$ ,  $\Lambda_{\text{RG}}$  and  $\Lambda_n$  models match well the observed growth rate and they provide good quality fits of the cosmological parameters at all redshifts. We remark that the power law model  $\Lambda_n$  behaves effectively as a scalar field model with an equation of state slightly tilted in the phantom DE regime ( $w < -1$ ). The idea that the models with a dynamical cosmological term  $\Lambda$  may behave effectively as quintessence or phantom DE has been described in general terms in the literature [22].
- (iii) The particular case of the RG model for  $n_0 = 0$  (or of the power series model for  $n_1 = 0$ ), i.e. the  $\Lambda_{H_1} = n_2 H^2$  model, is ruled out at a high significance level because the best parameter fit value for  $n_2$  is incompatible with the necessity of growing structure formation in this model.
- (iv) In the case of  $\Lambda$ ,  $\Lambda_{\text{RG}}$ , and  $\Lambda_n$  vacuum scenarios, the large scale structures (such as galaxy clusters) form later ( $z \sim 2$ ) with respect to those produced in the framework of the  $\Lambda_{\text{PS}_1}$  and  $\Lambda_{\text{PS}_2}$  models ( $z \geq 4$ ). Therefore, in view of the observational data, the former are much more favored as compared to the latter.
- (v) The expected redshift distribution of cluster-size halos in realistic future x-ray or SZ cluster surveys indicates that we will not be able to distinguish the closely resembling models (constant vacuum, quan-

tum field, and power-law vacuum) based on the evolution of cluster abundances using the first type of survey, but there is some limited hope with the second.

### ACKNOWLEDGMENTS

We are grateful to J. Grande for a careful reading of the manuscript and for useful discussions, and also to A. Avgoustidis for clarifying a point on model independent determinations of the cosmological parameters. We are indebted to F. R. Klinkhamer and G. E. Volovik for detailed correspondence on some of the theoretical motivations for the model that we have denoted  $\Lambda_{\text{PS}_2}$ . Last but not least, we are thankful to J. Fabris for reading the manuscript and for useful comments. J. S. has been supported in part by MEC and FEDER under project FPA2007-66665, by the Spanish Consolider-Ingenio 2010 program CPAN CSD2007-00042 and by DIUE/CUR Generalitat de Catalunya under project 2009SGR502. M. P. acknowledges funding by Mexican CONACyT grant 2005-49878.

### APPENDIX A: ALTERNATIVE VIEW OF THE BASIC COSMOLOGICAL EQUATIONS

The goal in this appendix is to give the reader the opportunity to appreciate the relative similarities and differences among the main time varying vacuum models ( $\Lambda_{\text{RG}}$ ,  $\Lambda_{\text{PS}_1}$ , and  $\Lambda_n$ ). In particular, we rewrite the basic cosmological equations in terms of a new set of formal cosmological parameters ( $\tilde{\Omega}_m$ ,  $\tilde{\Omega}_\Lambda$ ). In this new space, the basic structure of the  $\Lambda$ CDM Hubble flow (19) is more closely preserved, in the sense that it appears as the sum of  $\tilde{\Omega}_\Lambda$  times a function (which can just be one in some cases) and another term involving  $\tilde{\Omega}_m$  times another function. The two functions are normalized to one at present, so that the sum rule  $\tilde{\Omega}_m + \tilde{\Omega}_\Lambda = 1$  is fulfilled. The change of basis from the physical parameters ( $\Omega_m$ ,  $\Omega_\Lambda$ ) to the formal ( $\tilde{\Omega}_m$ ,  $\tilde{\Omega}_\Lambda$ ) ones involves additional parameters  $\gamma_i$  of the current model. The two parameter spaces coincide only if we can set the values of the  $\gamma_i$  such that the vacuum becomes static. Consider the following examples.

- (i)  $\Lambda_{\text{RG}}$  model: If we use Eq. (37), then the basic cosmological equations (see Sec. IV B) take the following forms:

$$H(t) = \sqrt{\tilde{\Omega}_\Lambda} H_0 \coth \left[ \frac{3H_0(1-\gamma)\sqrt{\tilde{\Omega}_\Lambda}}{2} t \right] \quad (\text{A1})$$

and

$$a(t) = \left( \frac{\tilde{\Omega}_m}{\tilde{\Omega}_\Lambda} \right)^{1/3(1-\gamma)} \sinh^{2/3(1-\gamma)} \left[ \frac{3H_0(1-\gamma)\sqrt{\tilde{\Omega}_\Lambda}}{2} t \right] \quad (\text{A2})$$

or

$$E^2(a) = \tilde{\Omega}_\Lambda + \tilde{\Omega}_m a^{-3(1-\gamma)}. \quad (\text{A3})$$

The scale factor at the inflection point is

$$a_I = \left[ \frac{(1-3\gamma)\tilde{\Omega}_m}{2\tilde{\Omega}_\Lambda} \right]^{1/3(1-\gamma)}. \quad (\text{A4})$$

Obviously, in the ( $\tilde{\Omega}_m$ ,  $\tilde{\Omega}_\Lambda$ ) basis, the above equations generalize more tightly those of the concordance  $\Lambda$  cosmology (see Sec. IV A) and reduce exactly to them for  $\gamma = 0$ .

- (ii)  $\Lambda_{\text{PS}_1}$  model: If we use Eq. (67), then the corresponding basic cosmological equations (see Sec. IV D) become:

$$H(t) = \tilde{\Omega}_\Lambda H_0 \frac{e^{\gamma\tilde{\Omega}_\Lambda H_0 t/2}}{e^{\gamma\tilde{\Omega}_\Lambda H_0 t/2} - 1} \quad (\text{A5})$$

and

$$a(t) = \left( \frac{\tilde{\Omega}_m}{\tilde{\Omega}_\Lambda} \right)^{2/\gamma} (e^{\gamma\tilde{\Omega}_\Lambda H_0 t/2} - 1)^{2/\gamma} \quad (\text{A6})$$

or

$$E(a) = \tilde{\Omega}_\Lambda + \tilde{\Omega}_m a^{-\gamma/2}. \quad (\text{A7})$$

Notice that in this particular case it is  $E(a)$ , rather than  $E^2(a)$ , which appears decomposed as a sum of two terms in the new parameter space. A perfect analogy with the  $\Lambda$ CDM Hubble flow is not always possible. Indeed, in this model the vacuum can never coincide with that of the standard model, except for the trivial (and excluded) situation where its energy is zero. The scale factor at the inflection point is given by

$$a_I = \left[ \frac{(\gamma-2)\tilde{\Omega}_m}{2\tilde{\Omega}_\Lambda} \right]^{2/\gamma}. \quad (\text{A8})$$

- (iii)  $\Lambda_n$  model: In this case we utilize Eq. (78). Therefore, the normalized Hubble flow obeys

$$E^2(a) = \tilde{\Omega}_m a^{-3} + \tilde{\Omega}_\Lambda a^{-n}, \quad (\text{A9})$$

while the corresponding inflection point is

$$a_I = \left[ \frac{\tilde{\Omega}_m}{(2-n)\tilde{\Omega}_\Lambda} \right]^{1/(3-n)}. \quad (\text{A10})$$

It is worth noting, that the current  $\Lambda_n$  cosmological model can be viewed as a classical *quintessence* model ( $P_Q = w\rho_Q$ , with  $w = -1 + n/3$ ), as far as the global dynamics is concerned. Since, however,  $n < 0$  (i.e.  $w < -1$ ) is preferred by the data, in practice it behaves effectively as phantom DE. The standard  $\Lambda$ CDM cosmology is recovered from this model in the limit  $n \rightarrow 0$  and  $\gamma = \Omega_\Lambda H_0^2/3$ .

**APPENDIX B: THE  $\Lambda_{\text{RG}}$  GROWTH FACTOR**

With the aid of the differential equation theory we present the growing model solution that is relevant to Eq. (40) for the RG model. Since the variable introduced in (38) satisfies  $y > 1$ , it is possible to find the solution  $D(y)$  of the differential Eq. (40) in terms of the associated Legendre functions of the second kind,  $Q_\nu^\mu(y)$ . The appropriate transformation reads as follows,

$$D(y) = (y^2 - 1)^{5-3\beta/6\beta} Q_\nu^\mu(y), \quad \nu = \frac{1}{3\beta}, \quad (\text{B1})$$

$$\mu = \nu - 1$$

where

$$Q_\nu^\mu(y) = C y^{-\nu-\mu-1} (y^2 - 1)^{\mu/2} F\left(a, b, c, \frac{1}{y^2}\right) \quad (\text{B2})$$

with  $a = 1 + \frac{\nu}{2} + \frac{\mu}{2}$ ,  $b = \frac{1}{2} + \frac{\nu}{2} + \frac{\mu}{2}$ ,  $c = \nu + \frac{3}{2}$ , and

$$C = e^{i\mu\pi} 2^{-\nu-1} \sqrt{\pi} \frac{\Gamma(\nu + \mu + 1)}{\Gamma(\nu + \frac{3}{2})}. \quad (\text{B3})$$

Inserting Eq. (B2) into Eq. (B1) and after some algebra we have

$$D(y) = C (y^2 - 1)^{1-\beta/6\beta} y^{-(2/3\beta)} F\left(\frac{1}{3\beta} + \frac{1}{2}, \frac{1}{3\beta}, \frac{1}{3\beta} + \frac{3}{2}, \frac{1}{y^2}\right) \quad (\text{B4})$$

or

$$D(y) = C (y^2 - 1)^{4-9\beta/6\beta} y F\left(\frac{1}{3\beta} + \frac{1}{2}, \frac{3}{2}, \frac{1}{3\beta} + \frac{3}{2}, -\frac{1}{y^2 - 1}\right) \quad (\text{B5})$$

where we have used the well-known linear transformation formula

$$F(\alpha, b, c, x) = (1 - x)^{-\alpha} F\left(a, c - b, c, \frac{x}{x - 1}\right). \quad (\text{B6})$$

Note that in our formulation the parameters become:  $\alpha = \frac{1}{3\beta} + \frac{1}{2}$ ,  $b = \frac{1}{3\beta}$ ,  $c = \frac{1}{3\beta} + \frac{3}{2}$ , and  $x = \frac{1}{y^2}$ .

**APPENDIX C: UNIFICATION OF THE VACUUM MODELS**

In this appendix we examine a more general class of vacuum models:

$$\Lambda = n_0 + n_1 H + n_2 H^2, \quad (n_0 \geq 0). \quad (\text{C1})$$

The time evolution equation for the Hubble flow is obtained by Eq. (4) as

$$\int_{+\infty}^H \frac{dy}{-\lambda y^2 + n_1 y + n_0} = \frac{t}{2} \quad (\text{C2})$$

where  $\lambda = 3 - n_2$ . If we assume that  $\lambda > 0$  (or  $n_2 < 3$ ) then corresponding general solution of Eq. (C2) is

$$H(t) = \frac{\rho_2 e^{\lambda(\rho_2 - \rho_1)t/2} - \rho_1}{e^{\lambda(\rho_2 - \rho_1)t/2} - 1} \quad (\text{C3})$$

and

$$a(t) = a_1 (e^{\lambda(\rho_2 - \rho_1)t/2} - 1)^{2/\lambda} e^{\rho_1 t} \quad (\text{C4})$$

where

$$\rho_{2,1} = \frac{n_1 \pm \sqrt{D}}{2\lambda} \rho_2 > \rho_1 \quad (\text{C5})$$

and  $D = n_1^2 + 4\lambda n_0 \geq 0$  is the discriminant.

Obviously, the  $\Lambda_{\text{PS}_{1,2}}$ ,  $\Lambda_{\text{RG}}$ , and  $\Lambda$  models are particular solutions of the general vacuum model. Indeed, we have

- (i) *Case 1:* If  $n_0 = 0$  then  $\rho_1 = 0$  and  $\rho_2 = n_1/\lambda$ . In this case, the basic cosmological equations [see Eqs. (C3) and (C4)] reduce to those found by either the  $\Lambda_{\text{PS}_1}$  (for  $\lambda = 3 - n_2 > 0$ ) or the  $\Lambda_{\text{PS}_2}$  (for  $\lambda = 3$ ) model, respectively, [see Eq. (51)].
- (ii) *Case 2:* If  $n_1 = 0$  then  $\rho_2 = -\rho_1$ . We select the unknown constants such as  $n_0 = 3\Omega_\Lambda H_0^2(1 - \gamma)$  and  $n_2 = 3\gamma$ . Therefore, the general Hubble expansion Eq. (C3), reduces to that derived by the  $\Lambda_{\text{RG}}$  model [see Eq. (24)].
- (iii) *Case 3:* If  $(n_1, n_2) = (0, 0)$  then  $\rho_2 = -\rho_1 = \sqrt{3n_0}/3$ . Thus, for  $n_0 = 3\Omega_\Lambda H_0^2$ , the Hubble expansion Eq. (C3), reduces to that derived by the concordance  $\Lambda$  cosmology [see Eq. (16)].

The analysis of structure formation for the model (C1) in the most general case when all the coefficients  $n_i$  are nonvanishing cannot be performed analytically. We shall report on this case elsewhere [78].

[1] D.N. Spergel *et al.*, *Astrophys. J. Suppl. Ser.* **170**, 377 (2007).  
 [2] T.M. Davis *et al.*, *Astrophys. J.* **666**, 716 (2007).  
 [3] E. Komatsu *et al.*, *Astrophys. J. Suppl. Ser.* **180**, 330 (2009).

[4] M. Tegmark *et al.*, *Astrophys. J.* **606**, 702 (2004).  
 [5] M. Hicken *et al.*, *Astrophys. J.* **700**, 1097 (2009).  
 [6] M. Kowalski *et al.*, *Astrophys. J.* **686**, 749 (2008).  
 [7] S. Weinberg, *Rev. Mod. Phys.* **61**, 1 (1989).  
 [8] P.J. Peebles and B. Ratra, *Rev. Mod. Phys.* **75**, 559 (2003).

- [9] T. Padmanabhan, *Phys. Rep.* **380**, 235 (2003).
- [10] L. Perivolaropoulos, arXiv.0811.4684.
- [11] P.J. Steinhardt, in *Critical Problems in Physics*, edited by V.L. Fitch, D.R. Marlow, and M.A.E. Dementi (Princeton University Press, Princeton, 1997); *Phil. Trans. R. Soc. A* **361**, 2497 (2003).
- [12] C.A. Egan and C.H. Lineweaver, *Phys. Rev. D* **78**, 083528 (2008).
- [13] A.D. Dolgov, in *The Very Early Universe*, edited by G. Gibbons, S.W. Hawking, and S.T. Tiklos (Cambridge University Press, Cambridge, England, 1982); R.D. Peccei, J. Solà, and C. Wetterich, *Phys. Lett. B* **195**, 183 (1987); C. Wetterich, *Nucl. Phys.* **B302**, 668 (1988); P.J.E. Peebles and B. Ratra, *Astrophys. J.* **325**, L17 (1988); J. Solà, *Phys. Lett. B* **228**, 317 (1989); C. Wetterich, *Astron. Astrophys.* **301**, 321 (1995).
- [14] J. Grande, J. Solà, and H. Štefančić, *J. Cosmol. Astropart. Phys.* **08** (2006) 011; *Phys. Lett. B* **645**, 235 (2007).
- [15] S. Basilakos, arXiv0901.3195.
- [16] B. Ratra and P.J.E. Peebles, *Phys. Rev. D* **37**, 3406 (1988); M.S. Turner and M. White, *Phys. Rev. D* **56**, R4439 (1997); R.R. Caldwell, R. Dave, and P.J. Steinhardt, *Phys. Rev. Lett.* **80**, 1582 (1998).
- [17] H.K. Jassal, J.S. Bagla, and T. Padmanabhan, *Phys. Rev. D* **72**, 103503 (2005); *Mon. Not. R. Astron. Soc.* **356**, L11 (2005).
- [18] L. Samushia and B. Ratra, *Astrophys. J.* **650**, L5 (2006); **680**, L1 (2008).
- [19] J.Q. Xia, H. Li, G.B. Zhao, and X. Zhang, *Phys. Rev. D* **78**, 083524 (2008); G.B. Zhao, J.Q. Xia, B. Feng, and X. Zhang, *Int. J. Mod. Phys. D* **16**, 1229 (2007); J.Q. Xia, G.B. Zhao, B. Feng, H. Li, and X. Zhang, *Phys. Rev. D* **73**, 063521 (2006).
- [20] J. Simon, L. Verde, and R. Jiménez, *Phys. Rev. D* **71**, 123001 (2005).
- [21] E.J. Copeland, M. Sami, and S. Tsujikawa, *Int. J. Mod. Phys. A* **15**, 1753 (2006).
- [22] J. Solà and H. Štefančić, *Phys. Lett. B* **624**, 147 (2005); *Mod. Phys. Lett. A* **21**, 479 (2006); *J. Phys. A* **39**, 6753 (2006).
- [23] F. Bauer, J. Solà, and H. Štefančić, *Phys. Lett. B* **678**, 427 (2009).
- [24] B.L. Nelson and P. Panangaden, *Phys. Rev. D* **25**, 1019 (1982); E.S. Fradkin and A.A. Tseytlin, *Nucl. Phys.* **B201**, 469 (1982); S.L. Adler, *Rev. Mod. Phys.* **54**, 729 (1982).
- [25] D.J. Toms, *Phys. Lett.* **126B**, 37 (1983); L. Parker and D.J. Toms, *Phys. Rev. D* **32**, 1409 (1985); I.L. Buchbinder, *Fortschr. Phys.* **34**, 605 (1986).
- [26] I.L. Shapiro and J. Solà, *Phys. Lett. B* **475**, 236 (2000); *J. High Energy Phys.* **02** (2002) 006; A. Babić, B. Guberina, R. Horvat, and H. Štefančić, *Phys. Rev. D* **65**, 085002 (2002); **71**, 124041 (2005).
- [27] A. Bonanno and M. Reuter, *Phys. Rev. D* **62**, 043008 (2000); **65**, 043508 (2002).
- [28] M. Ozer and O. Taha, *Nucl. Phys.* **B287**, 776 (1987); O.K. Freese *et al.*, *Nucl. Phys.* **B287**, 797 (1987); O. Bertolami, *Nuovo Cimento B* **93**, 36 (1986).
- [29] J.C. Carvalho, J.A.S. Lima, and I. Waga, *Phys. Rev. D* **46**, 2404 (1992); I. Waga, *Astrophys. J.* **414**, 436 (1993); J. Salim and I. Waga, *Classical Quantum Gravity* **10**, 1767 (1993); A.I. Arbab, *Gen. Relativ. Gravit.* **29**, 61 (1997).
- [30] J.M. Overduin and F.I. Cooperstock, *Phys. Rev. D* **58**, 043506 (1998); O. Bertolami and P.J. Martins, *Phys. Rev. D* **61**, 064007 (2000); J.S. Alcaniz and J.M.F. Maia, *Phys. Rev. D* **67**, 043502 (2003); R. Opher and A. Pelinson, *Phys. Rev. D* **70**, 063529 (2004); J.D. Barrow and T. Clifton, *Phys. Rev. D* **73**, 103520 (2006); Jr. Montenegro and S. Carneiro, *Classical Quantum Gravity* **24**, 313 (2007).
- [31] F. Bauer, *Classical Quantum Gravity* **22**, 3533 (2005);
- [32] I.L. Shapiro, J. Solà, C. España-Bonet, and P. Ruiz-Lapuente, *Phys. Lett. B* **574**, 149 (2003); C. España-Bonet, P. Ruiz-Lapuente, I.L. Shapiro, and J. Solà, *J. Cosmol. Astropart. Phys.* **02** (2004) 006; I.L. Shapiro and J. Solà, *Nucl. Phys. B, Proc. Suppl.* **127**, 71 (2004);
- [33] P. Wang and X. Meng, *Classical Quantum Gravity* **22**, 283 (2005); J.S. Alcaniz and J.A.S. Lima, *Phys. Rev. D* **72**, 063516 (2005).
- [34] L. Amendola, *Phys. Rev. D* **62**, 043511 (2000); W. Zimdahl, D. Pavón, and L.P. Chimento, *Phys. Lett. B* **521**, 133 (2001); L. Amendola, C. Quercellini, D. Tocchini-Valentini, and A. Pasqui, *Astrophys. J.* **583**, L53 (2003); G. Mangano, G. Miele, and V. Pettorino, *Mod. Phys. Lett. A* **18**, 831 (2003); R.G. Cai and A. Wang, *J. Cosmol. Astropart. Phys.* **03** (2005) 002; J.B. Binder and G.M. Kremer, *Gen. Relativ. Gravit.* **38**, 857 (2006); S. Das, P.S. Corasaniti, and J. Khoury, *Phys. Rev. D* **73**, 083509 (2006); G. Huey and B.D. Wandelt, *Phys. Rev. D* **74**, 023519 (2006); R. Mainini and S. Bonometto, *Phys. Rev. D* **74**, 043504 (2006); B. Wang, C-Y. Lin, and E. Abdalla, *Phys. Lett. B* **637**, 357 (2006); G.M. Kremer, *Gen. Relativ. Gravit.* **39**, 965 (2007); A.W. Brookfield, C. van de Bruck, and L.M.H. Hall (2007); G. Olivares, F. Atrio-Barandela, and D. Pavón, *Phys. Rev. D* **77**, 063513 (2008); J.-H. He and B. Wang, *J. Cosmol. Astropart. Phys.* **06** (2008) 010.
- [35] I.L. Shapiro, J. Solà, and H. Štefančić, *J. Cosmol. Astropart. Phys.* **01** (2005) 012.
- [36] J. Solà, *J. Phys. A* **41**, 164066 (2008).
- [37] D.J. Eisenstein *et al.*, *Astrophys. J.* **633**, 560 (2005); N. Padmanabhan *et al.*, *Mon. Not. R. Astron. Soc.* **378**, 852 (2007).
- [38] W.L. Freedman, *Astrophys. J.* **553**, 47 (2001).
- [39] M. Bronstein, *Phys. Z. Sowjetunion* **3**, 73 (1933).
- [40] R.C. Arcuri and I. Waga, *Phys. Rev. D* **50**, 2928 (1994).
- [41] J. Grande A. Pelinson, J. Solà, *Phys. Rev. D* **79**, 043006 (2009); arXiv:0904.3293.
- [42] J. Grande, R. Opher, A. Pelinson, and J. Solà, *J. Cosmol. Astropart. Phys.* **12** (2007) 007.
- [43] J.R. Bond, G. Efstathiou, and M. Tegmark, *Mon. Not. R. Astron. Soc.* **291**, L33 (1997).
- [44] S. Nesseris and L. Perivolaropoulos, *J. Cosmol. Astropart. Phys.* **01** (2007) 018.
- [45] S. Basilakos, S. Nesseris, and L. Perivolaropoulos, *Mon. Not. R. Astron. Soc.* **387**, 1126 (2008).
- [46] O. Elgaroy and T. Multamaki, *J. Cosmol. Astropart. Phys.* **9** (2007) 2; P.S. Corasaniti and A. Melchiorri, *Phys. Rev. D* **77**, 103507 (2008).
- [47] W. Chen and Y.-S. Wu, *Phys. Rev. D* **41**, 695 (1990).
- [48] R.G. Vishwakarma, *Classical Quantum Gravity* **17**, 3833 (2000); S. Ray, U. Mukhopadhyay, and X.H. Meng,

- Gravitation Cosmol. **13**, 142 (2007); A. Sil and S. Som, *Astrophys. Space Sci.* **318**, 109 (2008).
- [49] S. Carneiro, M. A. Dantas, C. Pigozzo, and J. S. Alcaniz, *Phys. Rev. D* **77**, 083504 (2008).
- [50] H. A. Borges, S. Carneiro, and J. C. Fabris, *Phys. Rev. D* **78**, 123522 (2008); H. A. Borges, S. Carneiro, J. C. Fabris, and C. Pigozzo, *Phys. Rev. D* **77**, 043513 (2008).
- [51] S. Basilakos, *Mon. Not. R. Astron. Soc.* **395**, 2347 (2009).
- [52] R. R. Caldwell, *Phys. Lett. B* **545**, 23 (2002); R. R. Caldwell, M. Kamionkowski, and N. N. Weinberg, *Phys. Rev. Lett.* **91**, 071301 (2003); A. Melchiorri, L. Mersini, C. J. Odman, and M. Trodden, *Phys. Rev. D* **68**, 043509 (2003); H. Štefančić, *Phys. Lett. B* **586**, 5 (2004); S. Nojiri and S. D. Odintsov, *Phys. Rev. D* **70**, 103522 (2004); R. J. Scherrer, *Phys. Rev. D* **71**, 063519 (2005); B. Feng, X. L. Wang, and X. M. Zhang, *Phys. Lett. B* **607**, 35 (2005); A. Vikman, *Phys. Rev. D* **71**, 023515 (2005); R. R. Caldwell and M. Doran, *Phys. Rev. D* **72**, 043527 (2005).
- [53] R. Schutzhold, *Phys. Rev. Lett.* **89**, 081302 (2002).
- [54] F. R. Klinkhamer and G. E. Volovik, *Phys. Rev. D* **79**, 063527 (2009); E. C. Thomas, F. R. Urban, and A. R. Zhitnitsky *J. High Energy Phys.* 08 (2009) 043.
- [55] F. R. Urban and A. R. Zhitnitsky, arXiv:0906.2162; *Phys. Rev. D* **80**, 063001 (2009); arXiv:0906.3546.
- [56] A. Avgoustidis, L. Verde, and R. Jiménez, *J. Cosmol. Astropart. Phys.* 06 (2009) 012.
- [57] P. J. E. Peebles, *Principles of Physical Cosmology* (Princeton University Press, Princeton, New Jersey, 1993).
- [58] I. L. Shapiro, *Classical Quantum Gravity* **25**, 103001 (2008); I. L. Shapiro and J. Solà, arXiv:0808.0315.
- [59] F. R. Klinkhamer and G. E. Volovik, arXiv:0905.1919.
- [60] J. C. Fabris, I. L. Shapiro, and J. Solà, *J. Cosmol. Astropart. Phys.* 02 (2007) 016.
- [61] A. M. Velasquez-Toribio, arXiv:0907.3518.
- [62] Lixin Xu, arXiv:0906.1113.
- [63] V. Silveira and I. Waga, *Phys. Rev. D* **50**, 4890 (1994).
- [64] S. Nesseris and L. Perivolaropoulos, *Phys. Rev. D* **77**, 023504 (2008).
- [65] L. Verde *et al.*, *Mon. Not. R. Astron. Soc.* **335**, 432 (2002).
- [66] E. Hawkins *et al.*, *Mon. Not. R. Astron. Soc.* **346**, 78 (2003).
- [67] M. Tegmark *et al.*, *Phys. Rev. D* **74**, 123507 (2006).
- [68] N. P. Ross *et al.*, *Mon. Not. R. Astron. Soc.* **381**, 573 (2007).
- [69] N. P. Ross *et al.*, *Mon. Not. R. Astron. Soc.* **381**, 573 (2007).
- [70] P. McDonald *et al.*, *Astrophys. J.* **635**, 761 (2005).
- [71] W. H. Press and P. Schechter, *Astrophys. J.* **187**, 425 (1974).
- [72] P. J. E. Peebles, *Astrophys. J.* **284**, 439 (1984); S. Weinberg, *Phys. Rev. Lett.* **59**, 2607 (1987).
- [73] D. Richstone, A. Loeb, and E. L. Turner, *Astrophys. J.* **393**, 477 (1992).
- [74] C. G. Lacey and S. Cole *Mon. Not. R. Astron. Soc.* 262, 627 (1993). V. Eke, S. Cole, and C. S. Frenk, *Mon. Not. R. Astron. Soc.* **282**, 263 (1996).
- [75] A. Jenkins *et al.*, *Mon. Not. R. Astron. Soc.* **321**, 372 (2001).
- [76] D. Reed, R. Bower, C. Frenk, A. Jenkins, and T. Theuns, *Mon. Not. R. Astron. Soc.* **374**, 2 (2007).
- [77] C. Fedeli, L. Moscardini, and S. Matarrese, arXiv:0904.3248.
- [78] S. Basilakos, J. Grande, M. Plionis, and J. Solà (unpublished).